USING LNS8801, A GPER AGONIST, TO TREAT GRM1^{+} MELANOMA IN A TRANSGENIC MOUSE MODEL

By

CHRISTINA N. MARINARO

A thesis submitted to the

School of Graduate Studies

Rutgers, The State University of New Jersey

In partial fulfillment of the requirements

For the degree of

Master of Science

Graduate Program in Microbiology and Molecular Genetics

Written under the direction of

Suzie Chen

And approved by

_____

_____

_____

New Brunswick, New Jersey

October, 2020

ABSTRACT OF THE THESIS

Using LNS8801, a GPER Agonist, to Treat GRM1^{+} Melanoma in a Transgenic Mouse Model

By, CHRISTINA N. MARINARO

Thesis Director:

Suzie Chen

Melanoma is the most aggressive form of skin cancer. The American Cancer Society estimated that over 100,000 new cases will be diagnosed and there will be over 7,000 deaths from the disease in 2020. There are several signaling pathways critical for the onset and progression of this deadly disease. The sex hormone, estrogen, has been shown to act directly on melanocytes through G-protein coupled estrogen receptors (GPER). This interaction results in increased pigmentation and differentiation in melanocytes to establish a protective effect against cellular transformation. The activation and subsequent signaling cascades associated with GPER are unique to melanocytes and do not overlap with the classical estrogen pathways. Linnaeus Therapeutics Inc. has identified and isolated a unique isomer, LNS8801 as the active component of the GPER agonist G-1. Previous studies with LNS8801 in melanoma allograft mouse models

showed a reduction in tumor progression and a lasting protective activity upon secondary challenge of the same tumor cells.

Our lab was the first to show that ectopic expression of a normal neuronal receptor, metabotropic glutamate receptor 1 (mGluR1/GRM1) in melanocytes is sufficient to transform cells *in vitro* and induce tumors *in vivo.* We established two transgenic mouse models, TG-3 and TGS, with aberrant GRM1 expression that develop metastatic melanoma spontaneously with 100% penetrance. In this project we propose to use the unique TGS mouse model and treat the animals with LNS8801 over 32 weeks to see the consequences of activated GPER. Furthermore, to emulate exposure to the natural carcinogen, UV radiation, most people endure every day, we will expose mice to UV throughout the study. Possible alterations in disease progression will be monitored by a small animal imaging system (IVIS). Several key protein markers shown earlier to be involved in GPER signaling will be evaluated by Western blots in excised tumor tissue samples. Finally, cytokine analysis will also be performed to examine possible changes in levels of cytokines, two specific ones, interlukin-10 (IL-10) and interferon gamma (IFN-γ), shown in previous investigations.

ACKNOWLEDGEMENT

I want to first and foremost thank Dr. Suzie Chen for all of her guidance and especially her patience over that last three years. You have taught me far more about both science and life than I could have ever imaged. It truly has been a pleasure to work for you. I am looking forward to staying on in the lab and seeing what other projects you have for me.

Next, I must thank my family and friends for their love and support, without all of you this would not have been possible. To my parents, you have both been my rock during this process. Thank you for always encouraging me in life and especially in this journey. To my brother, thank you for always finding a way to make me laugh and put a smile on my face even after a tough day in the lab.

Finally, I would like to thank current and past members of the Chen lab for their advice and guidance. Raj and Kevinn, thank you for the insight you have shared and skills you have taught me. John, an extremely big thank you for helping me with the image quantifications and animal work in this project. You have all made our lab such a fantastic place to work and learn.

TABLE OF CONTENTS

LIST OF FIGURES

INTRODUCTION

A. Melanoma

Melanoma is a highly aggressive form of skin cancer that without treatment can metastasize to vital organs and become deadly. In 2020 it is estimated that there will be 100,350 new cases and 6,850 deaths due to the disease (Siegel *et al.*, 2020). While being one of the rarest forms of skin cancer, only 3 percent of all cases are melanoma, it accounts for 90% of skin cancer deaths. There are multiple genetic and/or environmental risk factors that increase the likelihood of developing melanoma such as chronic sun exposure, family history, having a suppressed immune system and skin pigmentation. Melanoma arises from the transformation of melanocytes, the cells responsible for producing pigment in the skin, found in the basal layer of the skin (Dzwierzynski, 2013).

Many individuals have dark spots on their skin called nevi. These are non-cancerous but have the potential to transform if mutations to the melanocytes occur. UV radiation is the most common and preventable factor that causes DNA damage to melanocytes leading to their transformation. Nevi are typically found in a state of cellular senescence meaning they are not growing or dividing. DNA damage can cause a disruption to this senescence and promote the melanocytes in the nevi to begin rapidly dividing, become transformed and in some cases additional mutations occur (Ha *et al.*, 2008).

Disruption of cellular senescence has been attributed to mutation in both oncogenes and tumor suppressor genes. Oncogenes acquire gain of function mutations that lead to the formation of tumors. Two of the most commonly mutated oncogenes in

melanoma are *BRAF* and *N-RAS.* Mutations in one excludes mutations in the other and in either case leads to the enhanced stimulation of the mitogen-activated protein kinase signaling pathway (MAPK). Activation of MAPK pathway results in increased uncontrolled cellular proliferation. The most common *BRAF* (V600E), a single base mutation at codon 600 with valine substituted by glutamate is found in both melanomas and in benign nevi. It is not clear if melanomas originated from mutated *BRAF* nevi with additional mutations. Results from a genetically engineered mouse model showed the development of melanoma in melanocytes with mutated *BRAF* only when a tumor suppressor, Phosphatase and Tensin homolog, PTEN, was deleted (Dankort *et al*., 2009), suggesting mutated *BRAF* by itself was not sufficient to drive tumorigenesis. Other well-known tumor suppressors such as p53 were not frequently associated with melanomagenesis.

There are additional cascades that have been shown to be critical players in melanoma development including the phosphatidylinositide 3-kinase/AKT (PI3K/AKT) pathway. Activation of this pathway leads to increased cell survival. Due to mutations in this pathway melanoma cells can evade apoptosis and continue to survive and divide uncontrolled (McCubrey *et al.,* 2012). Another major pathway associated with melanoma development involves the tumor suppressor protein cyclin dependent kinase inhibitor 2A (CDKN2A). Loss of function mutations in this pathway, specifically in $P16^{INK4a}$ and p14 allows cells to bypass cell cycle checkpoints. In bypassing these checkpoints cells go right into G1 and uncontrolled cell growth occurs (de Araújo *et al*., 2016). These three hallmarks of cancer: uncontrolled proliferation, evasion of cell death and uncontrolled cell death, all contribute to the highly aggressive nature of melanoma.

B. Metabotropic Glutamate Receptor 1

Metabotropic glutamate receptors (mGluR) are membrane bound seven-transmembrane domain receptors that belong to the G protein-coupled receptor (GPCR) family with glutamate as their natural ligand. Glutamate is the major excitatory neurotransmitter in the central nervous system (CNS) (Meldrum, 2000). Binding of glutamate to a mGluR stimulates the receptor and concurrent activation of downstream signaling cascades. There are three groups of mGluRs, metabotropic glutamate receptor 1 (protein-mGluR1/gene-GRM1) belongs to the group 1 mGluRs that are couple with heterotrimeric subunits, Gα, G_{β} and G_{γ} proteins. Glutamate-stimulated activation of mGluRs causes a conformational change in the extracellular domains that catalyze the exchange of GTP for a GDP on the Gα and uncouples G_{α} from $G_{\beta\gamma}$ and activates Phospholipase C (PLC). PLC in turn hydrolyzes phosphatidylinositol (4.5)-biphosphate (PIP2) into diacylglycerol (DAG) and inositol 1,4,5-triphosphate to act as secondary messengers (Taylor *et al.,* 1991). Calcium is then released into the cytosol after stimulation by IP3 and DAG, the release of calcium activates protein kinase C (PKC) (Taylor *et al.,* 1991; Lüscher *et al.,* 2010). Active PKC causes a phosphorylation cascade that activates two of the signaling pathways, MAPK and PI3K/AKT, that play critical roles in cell transformation and tumorigenesis (Schonwasser *et al.,* 1998).

Metabotropic glutamate receptor 1 is normally expressed and functions in the central nervous system in memory and learning (Ménard, *et al.,* 2012). It also has been shown to play a role in multiple neurological diseases. Some of the most common diseases are amyotrophic lateral sclerosis (ALS), Huntington's disease and Alzheimer's disease (M Ribeiro *et al.,* 2010). Upregulation of both mGluR1 and mGluR5 (another

mGluR in group 1) is proposed as a possible mechanism for the degeneration of motor neurons in ALS (Battaglia and Bruno, 2018). Multiple studies have shown that GRM1 expression is not limited to the CNS and is expressed in several other tissues in the body (Lumen *et al.*, 2016). When this receptor is expressed outside of the CNS sometimes it acts as an oncogene promoting the transformation of normal cells to tumor cells (Zhao *et al.*, 2011).

C. Metabotropic Glutamate Receptor 1 in Melanoma

Overexpression or ectopic expression of mGluRs in various cell types can lead to their transformation. In order to ensure the constitutive activation of the receptor, autocrine/paracrine loops are formed (Takayama *et al.*,2017). These autocrine/paracrine loops in cells are formed with the Cystine/Glutamate antiporter xCT and mGluRs (Lyons *et al.*, 2007). The antiporter xCT facilitates the import of cystine and export of glutamate to the extracellular environment at a 1:1 ratio (Bannai, 1986). Cells require cystine which is then reduced to cysteine and participates in glutathione synthesis. Glutathione is critical in the reduction of toxic reactive oxygen species (ROS) in cells from many forms of stress (Sato *et al.*, 1999). Due to rapid cell growth and proliferation cancer cells often have high levels of ROS. High levels of ROS in cancer cells leads to constitutive xCT activation in order to keep the cells from undergoing cell death. Export of glutamate into the extracellular environment via xCT provides an abundance of ligand for mGluRs.

Our lab was the first to show the involvement of ectopic expression of GRM1 in normal melanocytes results in their transformation *in vivo* and *in vitro* (Pollack *et al.*, 2003). Spontaneous melanoma was first noted in transgenic mice generated with Clone B DNA. Clone B DNA is a 2-kb genomic DNA fragment which causes cells to undergo

adipocyte differentiation *in vitro* (Chen *et al.,* 1989; Colón-Teicher *et al.,* 1993). Integration of this transgene causes concomitant deletion of host DNA that was subsequently identified as intron 3 of the gene encoding GRM1. A classical case of insertional mutagenesis that led to the ectopic expression of mGluR1 in melanocytes and the spontaneous development of melanoma (Pollock *et al.,* 2003). These transgenic mice, TG-3 show heritable melanoma with 100% penetrance. This was further confirmed by targeted mGLuR1 expression to melanocytes only and the second transgenic line, Tg(Grm1)EPv (E) display similar onset and progression of melanoma as TG-3 (Pollock *et al.,* 2003). To facilitate the monitoring of tumor progression, TG-3 was crossed with a hairless SKH1 to yield TGS (Benavides *et al.,* 2009). TGS have a normal immune system and display pigmented lesions throughout the body which can be easily visualized and imaged due to the lack of fur. TGS also show similar onset and progression of tumor as TG-3 mice.

In vitro validation that GRM1 is an oncogene was demonstrated with GRM1 positive cells lines that were developed by transfecting mouse melanocytes (MelanA from C57BL/6) with GRM1 cDNA (Shin *et al.,* 2008). These GRM1 expressing cell lines have constitutive activation of the MAPK pathway. When these cells were inoculated into immunodeficient nude or syngeneic C57/BL6 mice, they formed large and invasive tumors as compared to the original vector transfected cells (Shin *et al.,* 2008). Taken together, these results showed that GRM1 expression in normal mouse melanocytes was sufficient to drive cell transformation *in vitro* and tumor formation *in vivo.*

Progenies of heterozygous (harbor only one disrupted copy of the transgene) TGS mice yield three genotypes: wild type that do not have the transgene and will not develop

any lesions, heterozygous mice that have one copy of the transgene and will develop lesions and homozygous which have two copies of the transgene and will also develop lesions. The major difference between heterozygous and homozygous mice is timing of the onset of melanoma. Heterozygous mice experience melanoma onset around 4-5 months where homozygous onset is around 4-6 weeks. This difference in disease onset also affects life expectancy with heterozygous mice living around 12-15 months before the tumor burden becomes too high where homozygous mice only survive about 4-5 months. Genotyping is confirmed via polymerase chain reaction (PCR) analysis of DNA collected from tail samples of the mice. For the purpose of the current long-term study only heterozygous TGS mice will be used.

D. Estrogen Signaling in Melanocytes is Mediated Through GPER

Studies as far back as fifty years ago have shown that female sex, history of multiple pregnancies and lower maternal age at an individual's first birth leads to decreased chance of melanoma and better prognosis when diagnosed, these results were later validated by multiple other groups (White, 1959). While the exact protective mechanism that is occurring is unknown it has been hypothesized that sex hormones, namely estrogen, are involved. Recent studies have shown that the activation and concurrent signaling of a G protein-couple receptor (GPCR), G-Protein Estrogen Receptor, GPER, (formerly known as GPR30) may be a factor in melanoma prevention and disease treatment. GPER is a seven-transmembrane G protein-coupled receptor that is located on the endoplasmic reticulum membrane (Revankar *et al.,* 2005).

Higher levels of estrogen were shown to increase both the pigmentation and differentiation in melanocytes. Primary human melanocytes increase in melanin

expression when treated with estrogen at levels similar to those of pregnant woman. Not only does estrogen increase melanin production in melanocytes but it also decreases proliferation. This decrease in proliferation was observed to be dependent on basal levels of melanin within cells, higher levels of melanin are more sensitive to estrogen treatment than cells with lower basal levels of melanin (Natale *et al.*, 2016).

This increase in pigmentation and terminal differentiation in melanocytes is believed to cause the protective effect seen in previous studies preventing melanocytes from becoming melanomas. In melanocytes, melanocortin receptor 1 (MC1R), is responsible for regulating both pigmentation and differentiation. When MC1R is activated in melanocytes it leads to the production of cyclic adenosine monophosphate (cAMP). cAMP then activates protein kinase A (PKA) that phosphorylates and activates the cAMP response element-binding protein (CREB). CREB is a transcription factor that promotes transcription of microphthalmia-associated transcription factor (MITF). MITF is a master regulator that is responsible for the transcription for genes that are required for melanin synthesis such as tyrosinase (D'Orazio and Fisher, 2011).

Estrogen signaling in melanocytes is mediated entirely through GPER and the pathway is distinct from classical estrogen pathways (Filardo *et al.*, 2002). Both qRT-PCR and western blotting have shown the lack of classical estrogen receptors in melanocytes indicating that estrogen signaling must be mediated through another pathway. Using RNA-seq data and previous studies on cAMP signaling it was determined that GPER was the most probable receptor mediating these activities. Increases in melanin production via treatment with estrogen was completely lost when GPER was deleted with shRNA hairpins or CRISPR-CAS9 (Natale *et al.*, 2016). Taken

together, it is apparent the presence of GPER is vital to melanin production and melanocyte differentiation.

E. G-1 is a Selective Agonist of GPER

In order to determine the specificity of GPER signaling a specific agonist was needed that would not activate classical estrogen pathways. GPR30-specific compound 1, G-1, was the only compound found to consistently out compete estrogen binding to GPER. G-1 also known by the chemical name: (1-[4-(6-bromobenzo[1,3]dioxol-5yl)-3a,4,5,9b-tetrahydro-3H-cyclopenta [c]quinolin-8-yl]-ethanone) is a substituted dihydroquinoline. Binding affinity assays showed that G-1 has a higher binding affinity to GPER than classical estrogen ligands such as 17β-estradiol. G-1 also showed a low binding affinity towards both classical estrogen receptors ERα and ERβ. Thus G-1 is not only selective for G-1 but also competes with estrogen in binding to GPER (Bologa *et al.,* 2006).

G-1 possess a higher binding affinity for GPER even in the presence of ERα and ERβ. If GPER is not present treatment with G-1 will have no affect and will not activate classical estrogen pathways. Activation of GPER causes the mobilization of intracellular calcium. When COS7 cells (monkey kidney fibroblast-like cells), that lack GPER but possess ERα and ERβ, are treated with G-1 there is no mobilization of intracellular calcium proving G-1 specificity for GPER. Treatment with 17β-estradiol in COS7 cells however does show mobilization of intracellular calcium. Activation of all three receptors respectively (ERα, ERβ and GPER) activates PI3K and PIP3 accumulates in the nucleus. Accumulation of PIP3 in the nucleus amplifies PI3K signaling by recruiting the serine/threonine AGC kinase (AKT) and phosphoinositide-dependent protein kinase-1

(PDK1) resulting in increased cell survival (Manning and Toker, 2015). Only G-1 shows accumulation of PIP3 in the nucleus if GPER is expressed. G-1 possess a highly selective binding affinity for GPER even in the presence of other estrogen receptors. When estrogen is present G-1 will compete and bind to GPER at a much higher rate (Bologa *et al.,* 2006). Being able to selectively activate GPER will allow for better understanding of the role estrogen may have in some diseases and the underlying mechanism of its mode of action.

F. Using G-1 to Target GPER in Cancer Treatment

GPER plays a role in almost every major system in the body. The receptor can be found in multiple different cells types and its activation leads to rapid downstream signaling and transcription regulation (Prossnitz and Barton, 2011). Treatment with G-1 has proven beneficial in multiple different cancers such as breast, ovarian, carcinomas and melanoma. Activation of GPER was shown to promote a decrease in cell proliferation, disease regression and protection from secondary challenge of disease.

Activation of GPER via treatment with G-1 has induced IL-10 expression and secretion by $CD4^+$ T cells. IL-10 is a cytokine that plays an important role in the immune system. Many different cell types express IL-10 such as T regulatory cells, $CD4^+$ and $CD8^+$ T cells, B cells and natural killer cells (Hedrich and Bream, 2010). T cell response is mediated by T reg and Th17 cells. T reg and Th17 cells produce IL-10 during an immune response to keep the response under control and prevent any possible autoimmune issues (Maynard and Weaver, 2008). While there is an ongoing debate whether IL-10 production is pro or anti-tumor there is a large amount of evidence for the latter. IL-10 plays a major role in the memory development of $CD8^+$ T cells that are

responsible for recognizing and killing cancer cells (Foulds *et al.,* 2006). Natural killer cells have also been shown to be stimulated by increased IL-10 expression leading to anti-tumor activity (Lauw *et al.,* 2000).

Ex vivo studies have shown that treatment of male native T cells with G-1 results in an increase in the number of T cells producing IL-10. To make sure that G-1 treatment leads to the specific secretion of IL-10 cells were allowed to differentiate in the presence of G-1 and then the conditioned media was tested for other cytokines such as TNF-α, IFN-γ, IL-6 and IL-17A. In the presence of G-1, native T cells secrete three times more IL-10 than untreated cells plus there is no increase in the secretion of other cytokines. This specific increase in IL-10 secretion is mediated through the MAPK/ERK signaling pathway which can be induced by GPER activation (Brunsing and Prossnitz, 2011). The ability to use compounds to increase IL-10 production could lead to new improved treatment modalities to fight multiple cancers.

Adrenocortical carcinoma (ACC) is a rare and highly aggressive cancer found in the adrenal gland with the primary treatment of complete surgical resection and few other chemotherapeutic options (Dackiw *et al.*, 2001). G-1 treatment in ACC xenograft mouse models with human adrenocortical carcinoma H295R cells, resulted in decreased tumor volume and promoted cell cycle arrest in the G2 phase. In ACC cells, G-1 has the ability to induce internucleosomal DNA fragmentation which leads to PARP-1 cleavage and the release of Cytochrome C from the mitochondria into the cytosol. Release of Cytochrome C into the cytosol activates both caspase 9 and caspase 3/7 leading to apoptosis. G-1 treatment showed increase expression in PARP-1 cleavage, caspase 9 and caspase 3/7 and activation of ERK1/2 (Chimento *et al.,* 2015). Prolonged activation of ERK1/2 was

shown to induce apoptosis (Chen *et al.,* 2005). G-1 could prove to be a beneficial treatment for ACC patients who cannot tolerate harsh chemotherapies.

In 2020 it is estimated that breast cancer will be the most diagnosed cancer in women and result in the second most deaths in women in the United States (Siegel *et al.,* 2020). Over 50% of breast cancer patients have a high expression levels of GPER and these high expression levels correlate to a favorable prognosis in patients (Filardo *et al.,* 2006; Arias-Pulido *et al.,* 2010). Treatment with G-1 showed the ability to inhibit proliferation in both ER-negative (SKBr3) and ER-positive (MCF-7) breast cancer cells. Cell cycle arrest occurs in both cell lines at the G2/M-phase due to inhibition of the G2/M specific regulatory proteins cyclin B1 and Cdc2. This loss of cell cycle regulation is what leads to apoptosis. GPER's growth inhibition on these cell lines is transient, lasting between 48-72 hours, and is dependent on its expression level. As breast cancer progresses GPER expression decreases due to methylation in its promoter region but can be reversed when treated with DNA methyltransferase inhibitors such as 5-Aza-2'-deoxycytidine (5-Aza). When GPER is methylated the effects of G-1 are negated. Treatment of cells with 5-Aza in combination with G-1 results in growth inhibition of cells. These results indicated that when GPER is methylated it cannot be activated by G-1 (Weißenborn *et al.,* 2014). This data suggests that G-1 with its specificity to GPER could be a beneficial treatment in patients with early stage breast cancer or in combination with other treatments for later stages.

G-1 could soon prove to be a beneficial therapy for melanoma treatment due to its ability to halt the cell cycle and little to no side effects on normal cells. Treatment with G-1 decreases the amount of viable melanoma cells by inhibiting cellular proliferation

(Riberio *et al.,* 2017). It is important to note that both estrogen and G-1 effects on melanoma cells are mediated through GPER and that melanoma cell lines do not express a classical ER (Natale *et al.,* 2016). Both an increase in melanin production and cell cycle arrest are detected in melanomas that lack the specific oncodrivers BRAF (B16F10 cells) and those that have mutated $BRAF^{V600E}$ (YUMM1.7) cells. The efficacies of G-1 were proven to be independent of the immune system by another allograft study using YUMM1.7 cells ($Braf^{V600E/wt}$ $Pten^{-/-}$ $Cdkn2^{-/-}$) inoculated into immunodeficient nude mice (Natale *et al.,* 2018). One of the most common features in human cancer is an increase in c-myc levels that promotes cell proliferation, survival and evasion of the immune system (Schlagbauer-Wadl *et al.,* 1999). G-1 induced GPER signaling resulted in a decrease in c-myc expression levels and an increase in the melanocyte differentiation markers tyrosinase and MITF. In mice, systemic treatment with G-1 also lead to a sustained protective effect that restricted formation of new melanomas after tumor clearance and secondary challenge with the same melanoma cell line (Natale *et al.,* 2018).

Further investigation into G-1 uncovered that G-1 is a combination of two isomers, LNS8801 and LNS8812. Testing on multiple cancer cell lines revealed that the purified isomer LNS8801 is the active compound in G-1. Currently Linnaeus Therapeutics Inc. has a phase 1 clinical trial for treatment with LNS8801 in patients who have metastatic or unresectable melanoma and have shown disease progression while on anti-PD-1/PD-L1 therapy. A second clinical trial is also on going in collaboration with Merck. This clinical trial is in phase 2 and combines LNS8801 with pembrolizumab in patients who have advanced stage solid tumors. Information on LNS8801 and clinical trials comes from personal communication with individuals at Linnaeus Therapeutics Inc.

G. UV Radiation and Melanoma

UV radiation is one of the most common physical carcinogens that individuals come in contact with every day. While sunlight is critical for life to function on earth it also consists of extremely harmful UVB radiation. While this radiation is not strong enough to penetrate any deeper than our skin it still is detrimental to DNA and proteins (De Gruijl, 1999). Studies as far back as 1928 showed that UV-radiation's bactericidal effect comes from the UV absorption by DNA (Gates, 1928). As pollution increases it continuously depletes the Earth's ozone layer that is primarily responsible for absorbing the majority of UVB rays. If trends in pollution continue and individuals keep ignoring warnings by tanning without protection from the sun incidences of skin cancer across the globe will only continue to increase.

When UVB is absorbed into the skin it can create a wide variety of DNA damage leading to carcinogenesis. UV radiation causes lesions in DNA to occur between adjacent pyrimidines to form dimers. Two types of dimers can form: cyclobutane dimers that occur between two cytosines (pCC) or two thymines (pTT) and pyrimidine (6-4) pyrimidone photoproducts that form between two pyrimidines (Soehnge *et al.*, 1997). This DNA damage deregulates the cell cycle and promotes carcinogenesis.

One of the most commonly mutated genes in human skin cancer is the tumor suppressor p53 (Brash *et al.,* 1991). Tumor suppressor genes help regulate the cell cycle and keep normal cells from transforming. Exposure to UV radiation has been shown to lead to irreversible DNA damage in the p53 gene. In the case of the p53 gene, as is often the case for tumor suppressor genes, both alleles of the gene must be damaged in order to cause a total loss of function. In the case of many human melanomas it was found the one

or both alleles of the p53 gene contained more than one mutation that could be attributed to exposure to UV radiation (Soehnge, *et al.,* 1997). UV radiation may also contribute to the induction of melanoma through the apoptosis of keratinocytes. Keratinocytes release growth factors that modulate melanocytes in growth and pigmentation. When an individual is exposed to UV radiation for a long period of time, i.e. enough time to become sun burnt, the keratinocytes absorbing the UV radiation will undergo apoptosis. This loss of keratinocytes and growth factors can lead to the transformation of melanocytes (Šitum *et al.*, 2007).

H. UV Radiation and the Immune System

UV radiation does more than just cause DNA damage to our skin, it can also have effects on the immune system. It is well-known that UV radiation is able to trigger local immunosuppression in the skin (Fisher and Kripke, 1977). To be able to understand how UV radiation can produce immunosuppression it is important to understand how the immune system of the skin works. Dendritic cells called Langerhans cells (LCs) in the epidermis process foreign antigens. Some of the LCs will migrate to the draining lymph node and present the antigen to naïve T cells. Once in contact with LCs $CD4^+$ T cells will differentiate into T helper 1/T helper 2 (Th1/Th2) cells. Th1 cells secrete cytokines such as interferon-γ (IFN-γ), interlukin-2 (IL-2), IL-4 and IL-10 which all play roles in immune response. Cytotoxic $CD8^+$ T cells and T regulatory cells (T reg) may also become activated. These T cells will then migrate to the area of infection or damage and become effectors cells while also recruiting other immune cells to the area (Norval, 2006).

Local immunosuppression is due to UV radiation damaging and reducing the number of LCs in the epidermis (Toews *et al.,* 1980). With decreased numbers of LCs and the remaining ones are mostly damaged, antigens cannot be presented properly to other immune cells. UV radiation can also cause moderate systemic immunosuppression due to the release of immunosuppressive cytokines by keratinocytes such as IL-10. IL-10 interferes with LCs ability to present antigens to Th1 cells and stimulates T regulatory cells. If IL-10 migrates into the blood stream after it is released by keratinocytes it has the potential to suppress immune responses in other areas of the skin or body not in direct contact with UV radiation (Schwartz, 2005).

While the majority of UV radiation effects on the immune system are immunosuppressive it is also possible to initiate some immunoprotective effects. When UV radiation induces DNA damage, specifically pyrimidine dimers, DNA repair is initiated via nucleotide excision repair (NER). The dimer is excised from the DNA strand before it is repaired leaving DNA oligos consisting of these dimers behind (Wood, 1996). Accumulation of Thymine-Thymine dimer oligos (pTTs) left behind by NER was shown to induce a protective effect in melanocytes by increasing p53 activity and epidermal melanin (Eller *et al.*, 1994). It is possible that the high mutation burden brought on by UV radiation could assist the immune system to recognize the beginning of tumor formation earlier and more effectively. A high tumor mutational burden in patients was shown to have a better prognosis to immunotherapy treatment in some clinical trials for melanoma and non-small-cell lung cancer (Steuer and Ramalingam, 2018). UV radiation and its influence on the immune system is a topic intensely examined by many investigators with new information frequently. Though most consequences caused by UV

radiation are immunosuppressive in melanoma but there may be a few that also help its recognition and treatment

I. Current Melanoma Treatments

There are many ways to treat melanoma currently in practice. Early stages of melanoma are always treated successfully via surgical resection. When surgical resection cannot be performed or does not completely remove the melanoma other methods of therapy need to be considered such as targeted therapies with small molecule inhibitors, radiation, chemotherapy or immunotherapy. Radiation therapy has proven usual at both local and systematic level (Maverakis *et al*., 2015). Radiation can cause local activation of immune cells, such as cytotoxic $CD8^+$ T cells, to identify and attack tumor cells that leads to migration of these immune cells to distant sites to strike out any tumor cells that may have metastasized from the primary tumor (Demaria *et al*., 2004). Targeted mutated *BRAF* inhibitor such as Vemurafenib is possible to inhibit mutated *BRAF* so the MAPK pathway cannot be activated (Sosman *et al*., 2012). One of the most common issues with targeted therapies is onset of resistance in patients. Use of Vemurafenib in combination with surgical resection is now an FDA approved therapy in late stage melanoma patients.

Immunotherapy is currently the front-line treatment approach for late stage and metastatic melanoma patients. Ipilumumab is an FDA approved immunotherapy targeting cytotoxic T-lymphocyte-associated protein 4 (CTLA-4). When CTLA-4 on T cells binds its ligand, B7, on antigen presenting cells (APCs) it leads to the inhibition of T cell activation. Ipilumumab binds to CTLA-4 so that it cannot become activated and T cells do not enter a state of cell cycle arrest. Another two commonly used FDA approved immunotherapies for melanoma and multiple other cancers is anti-PD-1 and anti-PD-L1.

T cells express programmed death receptor 1 (PD-1) on the cells surface, tumor cells express programmed death ligand 1 (PD-L1) on their cell surface. When the receptor on T cells binds to the ligand on tumor cells it induces cell death in the T cell allowing the tumor cell to evade the immune system and continue to proliferate. Anti PD-1 antibodies such as nivolumab or pembrolizumab will bind to the PD-1 receptors on T cells so it cannot bind to PD-L1. Atzolzumab/avelumab/duvalumab is an anti PD-L1 antibody and it binds to PD-L1 on tumor cells so PD-1 receptors on T cells cannot bind to it (Maverakis *et al*., 2015). Immunotherapies are only effective in a subset of patients and combining two different antibodies are frequently toxic. Better and less toxic therapies for melanoma are still necessary.

MATERIAL AND METHODS

A. Animals

TGS animals used were derived in the Suzie Chen Lab at Rutgers University. For the purposes of this study only heterozygous, possessing one copy of the transgene, animals were used. TGS animals are a cross between the founder transgenic melanoma mouse model, TG-3 (Zhu *et al.,* 1998), and a hairless model, SKH (Benavides *et al.,* 2009).

B. Antibodies

C-Myc (1:200) and tyrosinase (1:200) antibodies were both purchased from Santa Cruz Biotechnology (Dallas, TX). MITF (1:1000), tubulin (1:10,000), anti-rabbit secondary (1:5,000), and anti-mouse secondary (1:5,000) were purchased from Millipore Sigma (Burlington, MA). Beta Actin (1:5,000), GPER (1:1,000) and anti-goat secondary (1:5,000) was purchased from Invitrogen (Waltham, MA). All antibodies were diluted in 0.25% milk in Tris buffered saline (TBST). TBST consists of 1.37M NaCl, 0.28M Tris Base pH 7.6 and 1% Tween20 (Millipore Sigma; Burlington, MA).

C. Blood collection and plasma separation

Mice were bled via retro-orbital bleeding using heparinized capillary tubes (Fisher Scientific Waltham, MA). Approximately 300uL was taken from each animal each time and kept on ice until further processing. Tubes with collected blood were centrifuged at 4ºC for 8 minutes at 1,000xg. The plasma supernatant was taken and stored at -20ºC until needed.

D. Cytokine analysis

Cytokine analyses for IL-10 and IFN-γ were performed with isolated blood plasma in 96-well plates using commercially available ELISA assay kits and following the manufacture's instruction. Mouse IL-10 ELISA assay kit was purchased from R&D Systems (Minneapolis, MN). IFN-γ ELISA kit was purchased from Millipore Sigma (Burlington, MA). Plates were read at 450nm on an Infinite 200 Pro purchased from Tecan (Mannedorf, Switzerland).

E. Genotyping

In order to confirm that all TGS animals used in this study were heterozygous for the transgene we performed genotyping via Polymerase Chain Reaction (PCR). Genomic DNA was isolated from tail samples using a Zymo *Quick*-DNA Miniprep Plus kit purchased from Zymo Research (Irvine, CA). DNA concentration was determined by electrophoresis of samples on 0.8% agarose gel. Genomic DNA was then diluted accordingly to prepare for PCR with RNase free water included in Qiagen Taq PCR Master Mix Kit (Venlo, Netherlands).

PCR was performed according to the Qiagen Taq PCR Master Mix Kit protocol. Diluted DNA samples were mixed with Qiagen Taq PCR Master Mix, RNase free water, reverse primer and forward primer. Two separate PCR reactions were carried out for each DNA sample, one to detect the undisrupted GRM1 intronic sequences and one to detect the border of host and inserted transgene.

The forward and reverse primer sequences are: GMNDD

(5’-GTTGAGTGATGACATCATATCT-3’) and GMNDR

(5’-ACCATACAAAACCACAATATC-3’) for the detection of the wild type GRM1 intronic sequences, the amplified sequence is approximately 1.1kbp. The other forward and reverse primer set sequences are: TG3F (5’-TCCATCCTAAACTAAGACACCCATA-3’) and TG3R

(5’-CAGTTTGTGTCAGTCTGTTCTCTG-3’) for the detection of the host/transgene junction, the amplified fragment is approximately 300bp. The PCR reaction is as follows: denaturing at 95ºC for 1 minute and 15 seconds, 94ºC for 45 seconds, annealing step at 63ºC for 45 seconds-1ºC per cycle, elongation step held at 72ºC for 4 minutes and this cycle is repeated thirteen times from the step at 94ºC for 45 seconds. After the cycle is repeated 13 times then the cycle denatures the DNA at 94ºC for 45 seconds, anneals the primer at 50ºC for 45 seconds, elongates at 72ºC for 4 minutes and adding 5 seconds every cycle for 29 cycles. After the 29 cycles are finished the last elongation step is 72ºC for 10 minutes. The PCR products were electrophoresed on 1.5% agarose gels. Presence of bands for both the transgene and the wild type gene indicates a heterozygous genotype.

F. Imaging by IVIS and lesion quantification by ImageJ software

TGS mice were imaged using IVIS Lumina LT series III from Caliper Life Sciences (Waltham, MA). Animals were anesthetized using vaporized isoflurane (1-3% continuous flow mixed with oxygen, Primal Critical Care; Telangana, India). Images were taken of the dorsal side of the animals and saved for quantification at a later time. To quantify tumors on the dorsal side of the animal four 50x50 pixel boxes were chosen at random and the same four boxes were followed throughout the study. We used ImageJ

software (provided by the NIH) to process and quantify pigmented lesions on the captured images. Both total and average tumor burden from calculated pigment pixels, along with the number of lesions, for each mouse was tracked throughout the study.

G. Statistical analysis

Statistical analysis was performed using StatPlus software, an extension of Microsoft Excel (AnalystSoft; Walnut, CA). Statistical significance was calculating using a one-way ANOVA with Bonferroni's correction. P values ≤ 0.05 are considered statistically significant.

H. Study design

For this study heterozygous animals were divided into two groups of 24, one exposed to UVB radiation and the other not exposed to UVB. Each group of 24 consists of 12 males and 12 females, 6 were given the vehicle (13% DMSO, 82% sesame oil and 5% 200 proof ethanol) and 6 were given LNS8801 (1mg/kg). LNS8801 was provided to us by Dr. Todd Ridky and colleagues at the Perelman School of Medicine, University of Pennsylvania. The lyophilized LNS8801 was reconstituted in DMSO to a concentration of 50mg/mL. Animals were treated three times a week for three consecutive days with freshly prepared 100uL of LNS8801 (1mg/kg) in of 13% DMSO, 82% sesame oil and 5% 200 proof ethanol or the respective vehicle. Once a week, animals in the UV group were subjected to 30mJ/cm^2 of UVB radiation using a UV light cabinet (Daavlin; Bryan, OH). IVIS images, body weights and blood were collected every four weeks in the group not exposed to UV. In the group that was exposed to UV body weight was taken every week and blood and images were taken every two weeks. At termination of the study at 32

weeks, tumor and normal skin samples, liver, lung, lymph nodes and brain were taken at necropsy for further study.

I. Tissue protein lysate

Frozen tissue samples were mechanically ground using a motor and pestle and kept cold with the addition of liquid nitrogen to prevent protein degradation. The sample was then poured into a 10mL snap cap tube where an appropriate amount of lysis buffer and phosphatase plus proteinase inhibitors were added depending on the size of the sample. This combination consists: 940uL lysis buffer, 10uL phosphatase inhibitor cocktail 2 (Millipore Sigma; Burlington, MA), 10uL phosphatase inhibitor cocktail 3 (Millipore Sigma; Burlington, MA), and 40uL protease inhibitor cocktail (Roche; Basel, SZ). The lysis buffer consists of 50mM Tris hydrochloride pH 7.75 (Millipore Sigma; Burlington, MA), 150nM sodium chloride (Millipore Sigma; Burlington, MA), 1mM ethylenediaminetetraacetic acid (Fisher Scientific; Waltham, MA), 5% glycerol (Fisher Scientific; Waltham, MA), 1% Igepal (Millipore Sigma; Burlington, MA) and 1mM Dithiotheritol (Millipore Sigma; Burlington, MA).

Once the sample and lysis buffer are in the snap cap tube a handheld homogenizer (OMNI International; Kennesaw, GA) was used to further grind up samples and mix with lysis buffer. After the tissue sample is homogenized, each tube is sealed with parafilm and allowed to rock at 4º C for two hours. At the end of the two hours each sample was transferred to an 1.5mL Eppendorf tube and centrifuged at 4º C for 20 minutes at 10,000xg. The centrifuged samples are separated into 3 layers: the pellet of debris, extracted protein, and DNA. The middle protein layer was taken and stored at -80ºC until needed.

J. Western blots

Western blot analysis was performed on protein lysate prepared from tissue samples by adding 1uL of 2-mercaptoethanol (Millipore Sigma; Burlington, MA) for every 5uL of lysate plus 1uL of 5x sample buffer (250mM Tris Hydrochloride pH7.75, 10% SDS and 0.05% bromophenol blue). 5x sample buffer was diluted to 1x with 85% glycerol and 9.8% 2-mercaptoethanol (Millipore Sigma; Burlington, MA). Samples were then heated at 95ºC for 5 minutes on a glycerol heat block and rapidly cooled for an additional 5 minutes before use in westerns.

10% SDS-PAGE (polyacrylamide gel electrophoresis) gels were used for electrophoresis at 120V for 2-3 hours in running buffer [10% 10x Tris glycine pH 7.6 (Tris base plus glycine) and 1% of 10% sodium dodecyl sulfate (SDS) solution in deionized water], depending on the sizes of the proteins of interest. A pre-stained protein ladder (10uL) from Thermo Fisher Scientific was used for reference of the molecular weights of proteins. The electrophoresed samples on the gel were transferred onto a nitrocellulose membrane at 4ºC for 2 hours at 160mAmps in 1x transfer buffer [10% Tris glycine pH7.6 (as described above, 0.1% of 10% SDS and 10% methanol]. Staining with ponceau red dye (Millipore Sigma; Burlington, MA) was used to visualize the transferred proteins. The membrane was then blocked in 5% milk in TBST (as described in the antibodies section) for one hour. After blocking, the membrane was incubated in their respective antibody overnight on a rocker at 4ºC. At the following day the membrane was washed twice with TBST and incubated in their respective secondary antibodies for 1 hour at room temperature. After the incubation with the secondary antibody the membrane was washed five times with TBST, a WesternSure pen (LI-COR Biosciences;

Lincoln, NE) is used to mark the ladder. The membrane is covered with Lumina Crescendo Western HRP substrate (Millipore Sigma; Burlington, MA). Tubulin was incubated in its primary antibody for 15 minutes at room temperature, washed twice with TBST and incubated with secondary antibody for 20 minutes at room temperature. After incubation with secondary antibody the membrane was washed five times with TBST, the protein was then marked with the WesternSure pen and the membrane was covered in HRP substrate. Imaging of membranes was done using GeneSys imaging software and bands were quantified using ImageJ software.

RESULTS

A. Reduced tumor progression only in animals treated with LNS8801 and exposed to UV radiation

Based on the exciting results shown by Natale and colleagues we decided to test the efficacy of the active isomer, LNS8801, of G-1 using our melanoma-prone transgenic mouse model, TGS, in a longitudinal study using only heterozygous TGS mice. The pigmented tumors on TGS mice are visible and can be used as a measurement of tumor progression. To achieve this unbiased measurement of tumor progression we took advantage of a small animal imaging system (IVIS). We initiated treatment with LNS8801 via oral gavage three times a week when the animals were 8 weeks old and continued for 32 weeks. Images and blood were collected every four weeks. To mimic the UV exposure that a person is exposed to throughout their daily life we set up one group of TGS to be subjected to UV radiation once a week at 30mJ/cm^2. Tumor progression monitored via IVIS was used to calculate tumor burden for each mouse. Tumor burdens were calculated with the images acquired by IVIS every four weeks and with ImageJ software the pigmented lesions are converted to pixels taking into account the size and degree of darkness of the pigmented lesions. Four 50x50 pixel boxes were randomly selected with the first image and the same boxes were used throughout the entire study. The calculated tumor burdens were used as a surrogate for tumor progression.

For the group not exposed to UV radiation tumor progression was significant in both the LNS8801 and vehicle treated groups when compared to the images from week 0 to week 32 (Figure 1). Equal number of males and females were used for the study, a

possible gender-biased responses was analyzed. No differences between tumor burden in male and female TGS mice was detected in either treatment with LNS8801 or vehicle (Figures 2 and 3). In contrast to the reported allograft studies we did not see any inhibition of tumor progression in our transgenic mouse model in a 32-week treatment period.

We then attempted to mimic exposure to UV (sun light) by people, we exposed the TGS mice at 8 weeks of age to UV radiation at 30mJ/cm^2. We selected this dosage based on our earlier studies where exposure to UV at 30mJ/cm^2 twice a week for 10 weeks led to a substantial increase in tumor burden and continued for another 12 weeks without additional UV exposure, suggesting "UV-induced" damage as indicated by enhanced tumor burden was lasting. Elevated levels of several inflammatory proteins including IL-1α, IL-1β, IL-6 and VEGF were noted (Chen and Huang, unpublished results).

A group of 8-week old TGS mice were exposed to UV at 30mJ/cm^2 once a week for 32 weeks and treatment with vehicle or LNS8801 by oral gavage three times a week for 32 weeks. IVIS images and blood were collected every four weeks. A significant increase in tumor burden in UV-exposed mice treated with either vehicle control or LNS8801 was detected (Figure 4). We then analyzed the data based on the genders of the animals. For male mice significant tumor burden progression was observed in both the vehicle control and LNS8801 (Figure 5). UV-exposed vehicle treated female mice showed a significant increase in tumor burden. In contrast, UV-exposed LNS8801 treated female TGS mice did not show a significant increase in tumor burden (Figure 6).

UV, a well-known environmental carcinogen has been proposed to contribute to skin cancer (De Gruijl, 1999). We compared tumor burden in TGS mice with or without UV exposure to see if UV exposure also elevated tumor burden in our mouse model. In UV-exposed male TGS mice, treatment with vehicle control led to a significantly higher tumor burden at the end of our studies compared to male TGS mice not exposed to UV (Figure 7). In contrast, UV-exposed TGS male mice given LNS8801 did not show significant increase in tumor burden at 32 weeks when compared to those not exposed to UV (Figure 7). For female TGS mice in the vehicle controls, no significant differences in tumor burden was detected when comparing non-UV to UV exposed mice at 32-weeks (Figure 8). Treatment with LNS8801 in UV-exposed TGS female mice had a significant reduction in tumor burden at 32 weeks compared to those not exposed to UV (Figure 8).

B. Cytokine analysis of circulating blood plasma of TGS mice treated with vehicle or LNS8801 with or without UV exposure

We were interested to assess the level of two major cytokines, IL-10 and IFN-γ, in the circulating blood plasma. Previous studies showed that the activation of GPER with G-1 leads to an increase in IL-10 levels (Hedrich and Bream, 2010). IL-10 is expressed by keratinocytes in the epidermis in the presence of a foreign antigen. Both T reg and Th17 cells are influenced by the expression of IL-10, aiding in the regulation of immune response and preventing an autoimmune reaction (Maynard and Weaver, 2008). An increase in IL-10 has also been shown to aid in the development of memory $CD8^+$ T cells and the stimulation of natural killer cells (Foulds *et al.,* 2006; Lauw *et al.,* 2000). We looked at IFN-γ for its influence on immune response to foreign antigen and tumor formation. When tumor cells are detected by the immune system various T cells become

activated. IFN-γ is secreted by Th1 cells and influences B cell proliferation and differentiation by selectively inhibiting or promoting which class of immunoglobulin is expressed. This response allows the immune system to react quickly and effectively (Snapper and Paul, 1987).

In order to see if these two cytokine levels were modulated by treatment with LNS8801 or UV exposure, blood plasma samples were collected from the mice throughout the studies at designated timepoints of every four weeks. Selected blood plasma samples were used to detect IL-10 and IFN-γ using ELISA analysis.

For both male and female mice in the absence of UV exposure and regardless of treatment with vehicle or LNS8801, a significant reduction in IL-10 levels in circulating blood plasma was observed when we compared week 0 with week 32 (Figure 9). In contrast, for male and female mice exposed to UV and treatment with vehicle control or LNS8801, no significant difference in IL-10 was detected (Figure 10).

For IFN-γ levels, in the absence of UV exposure, the only group that showed a significant increase in IFN-γ is female TGS mice treated with LNS8801 (Figure 11). With the addition of UV exposure, a more general overall increase in IFN-γ levels was detected in male TGS mice regardless of treatment with vehicle control or LNS8801 (Figure 12). For female TGS mice exposed to UV only those treated with LNS8801 showed a significant increase in IFN-γ (Figure 12).

C. Treatment with LNS8801 led to lower levels of c-myc in male mice

An increase in c-myc expression levels is a common hallmark for cancer because it correlates with an increase in cell proliferation (Schlagbauer-Wadl *et al.,* 1999).

Previous studies have found that upon treatment with G-1 *in vitro* using B16F10 (mouse melanoma) and WM46 (human melanoma) cells resulted in reduced c-myc levels (Natale *et al.,* 2018). We were interested to know if the decrease in c-myc expression level also takes place in our system with LNS8801. We collected ear and tail samples from the mice at designated timepoints and prepared protein lysates for Western Blot analysis.

In the absence of UV, the male TGS mice in both vehicle and LNS8801 treated groups showed an overall similar increase in c-myc levels over the 32-week treatment period (Figure 13). With UV exposure, the c-myc levels were similar in vehicle-treated group but lower in LNS8801treated TGS males (Figure 14). For female TGS mice, an overall increase in c-myc levels in both vehicle and LNS8801 treated mice (Figures 13 and 14). Some of the variability in c-myc levels may be contributed by a varying number and degree of tumor stages within individual pigmented lesions.

D. Tyrosinase levels vary upon treatment with LNS8801 *in vivo*

Tyrosinase gene plays a critical role in both melanocyte differentiation and pigmentation or melanin production. Melanin protects melanocytes from harmful UV radiation. A higher degree of melanocytic differentiation leads to a lower level of proliferation thus lower potential for tumor development (Jimbow *et al.,* 1975). The more pigmentation and differentiation a melanocyte has the less likely it is to transform into a melanoma. Previous *in vitro* studies in WM46 cells have shown an increase in melanin production and levels of tyrosinase upon treatment with G-1 (Natale *et al., 2016*; Natale *et al.,* 2018).

For tyrosinase, the levels fluctuated over the treatment period of 32 weeks but very little significant changes in either vehicle or LNS8801 treated groups in both genders (Figures 15 and 16). As seen in the c-myc western blots analysis tyrosinase varied throughout the timepoints. The protein lysates were prepared from a mixed ear tumors and tail tissue samples. Unless dissected individual pigmented lesions from each group are prepared for the analyses, the current results represent an overall assessment in the absence of significant alterations

E. Reduced MITF levels detected in TGS mice without exposure to UV

Microphthalmia-associated transcription factor (MITF) is the main regulator of melanocyte differentiation. MITF is responsible for upregulating transcription factors that activate genes, such as tyrosinase, that are required for melanin synthesis (D'Orazio and Fisher, 2011). Higher levels of MITF in melanocytes leads to a more differentiated population and increased melanin production preventing the transformation to melanoma. As with tyrosinase, previous *in vitro* studies in WM46 cells have shown an increase in MITF expression levels when cells are treated with G-1 (Natale *et al.*, 2018).

As in previous western blots analysis, protein lysates from tissue samples at varying timepoints were used. In both male and female animals not exposed to UV, there was a reduction in the levels of MITF (Figure 17). A significant increase in tumor burden over time was observed in both male and female TGS mice. It is possible that as the disease progressed, levels of MITF were reduced with less cell differentiation. For TGS females exposed to UV, there was very little modulation MITF levels over time. TGS males exposed to UV and treated with LNS8801 saw higher levels of MITF than vehicle controls (Figure 18). These results would suggest that while disease progression

decreases overall MITF expression treatment with LNS8801 is able to partially rescue MITF expression.

DISCUSSION

Melanoma accounts for a very small fraction of all skin cancers but it accounts for the majority of deaths contributed to skin cancer. In early stages, melanoma can be cured with great success by surgical resection, however, over more than half of the time the disease returns with extraordinary metastatic potential and frequently is resistant to most treatment modalities. Within the last few years, the treatment for metastatic melanoma has improved with the advent of targeted therapies and immunotherapies, however, resistance to targeted therapies is a frequent event and immunotherapies only benefit a subpopulation of patients. There is clearly a need for further investigation to identify additional treatment options.

The current project describes the study using our unique metastatic melanoma mouse model, TGS, and treatment with the agonist, LNS8801, of a G-protein coupled estrogen receptor GPER. We showed that after a treatment period of 32 weeks in both male and female TGS there was no statistically significant differential responses between vehicle controls and LNS8801. In an attempt to mirror the daily exposure to UV from sunlight, we added UV exposure to a group of TGS mice once a week for the duration of the studies. Statistically significant tumor progression was detected in UV-treated TGS mice, however, when the tumor burden data was divided according to gender, there was no statistically significant tumor growth in female TGS mice while the male TGS still display significant tumor progression. These results suggest that including UV exposure to TGS mice with treatment of LNS8801 promoted substantial anti-tumor progression only in female mice. These results are also supported by earlier studies that showed female mammals have a more robust immune system than males (Klein and Flanagan,

2016). Our observations also agreed with studies performed by Natale et al., where the use of the parent agonist G-1 in a melanoma cell allograft study led to reduced tumor volumes and extended survival in female mice (Natale *et al.*, 2018).

Comparison between TGS mice not exposed to UV versus those exposed to UV confirmed the notion that the well-known environmental carcinogen, UV, contributed to tumorigenesis in skin as evident by the increase in tumor burden, yielded interesting results. In the vehicle control TGS male mice, UV radiation led to significantly higher tumor burden at 32-weeks indicating UV radiation increases tumor burden. In LNS8801 treated UV-exposed TGS males there is an overall increase in tumor burden, however, the inclusion of UV exposure did not further augment tumor burden, suggesting that the inclusion of LNS8801 may have some "protective" activity in these mice. For vehicle control female TGS mice, tumor burden was similar regardless of the addition of UV exposure. However, when UV-exposed female TGS mice are treated with LNS8801, a substantial reduction in tumor burden is noted, suggesting that LNS8801 mediated "protective" properties in these mice.

Since LNS8801 is an agonist of estrogen it is possible that using LNS8801 in female mice that already have a high basal level of estrogen is a combination that yields a better response perhaps via GPER activation. GPERs not stimulated by LNS8801 could in turn be activated by native estrogen boosting the overall mode of action as evident by a decrease in the progression of tumors. Since males have a lower basal level of native estrogen, there is not as much estrogen to completely saturate the remaining GPERs that LNS8801 does not stimulate thus could not generate a robust impact in reducing tumor progression.

In addition to the possible additive influence by higher endogenous estrogen levels in female mice when exposed to UV, another possible contributor to reduced tumor progression is mutational burden. Earlier studies have shown that an increase in tumor mutational burden correlates with a better prognosis in some cancers (Eller *et al.,* 1994; Steuer and Ramalingam, 2018). The UV induced DNA damage to melanocytes may promote a boost in immune response locally in the skin by facilitating in recognition and destroying melanoma cells. When DNA is damaged due to UV, the nucleotide excision repair (NER) pathway is turned on. With NER free oligos consisting of pTT b to begin build up in the skin. Presence of these random pTT oligos has been shown to increase p53 activity and melanin production in melanocytes (Soehnge *et al.,* 1997). Elevated p53 and melanin production may also contribute our observation that better responses to LNS8801 in UV-exposed female TGS mice than other groups.

In contrary to previous studies, we did not see an increase in production of IL-10 when GPER is activated by G-1 (Hedrich and Bream, 2010). We showed that when mice are not exposed to UV and treated with either LNS8801 or vehicle there is a moderate yet significant decrease in IL-10 levels with time. IL-10 is expressed by $CD4^+$ T cells and natural killer cells (Hedrich and Bream, 2010). Secretion of IL-10 helps keep T reg cells under control, so autoimmunity does not occur (Maynard and Weaver, 2008). IL-10 has both immunosuppressive and immunostimulatory properties and is key in regulation of the immune system.

In contrast, mice that were treated with UV and either vehicle or LNS8801 did not show significant differences in IL-10 levels regardless of sex over time. IL-10 is secreted by keratinocytes in the epidermis. Keratinocytes in the epidermis are responsible for

absorbing and responding to the majority of UV we are exposed to every day. When keratinocytes absorb enough UV, they will undergo apoptosis and release intracellular IL-10. This release of intracellular IL-10 can lead to both a local and systemic immunosuppression if it reaches the lymph or blood stream (Schwartz, 2005). Despite being exposed to UV radiation plus treated with LNS8801 we did not see significant modulations in IL-10 levels of circulating blood plasma.

We then examined a second major cytokine IFN-γ. IFN-γ is secreted by Th1 cells after they come in contact with a foreign antigen. Once IFN-γ is secreted, it migrates to native B cells and influences both cell proliferation and differentiation. This process selectively inhibits or promotes which form of immunoglobulin will be expressed (Snapper and Paul, 1987). In TGS mice in the absence of UV but treatment with LNS8801 only in female mice exhibited a moderate increase in IFN-γ levels in circulating blood plasma. In contrast, with the addition of UV radiation elevated IFN-γ levels were detected in male mice regardless treatment with vehicle or LNS8801. In female TGS mice an increase in IFN-γ levels was only observed in LNS8801 treated ones regardless of UV exposure. It is possible that the UV-induced increased DNA damage and cellular apoptosis promotes a more robust immune response as manifest by higher IFN-γ.

We next looked at several melanocyte specific markers in cell differentiation and pigmentation including c-myc, tyrosinase and MITF. In many cancers, including melanoma, levels of c-myc increase. Higher levels of c-myc positively correlate to increased cellular proliferation (Schlagbauer-Wadl *et al.,* 1999). Tyrosinase plays major role in both melanocyte differentiation and melanin production. Melanin helps protect

melanocytes from UV damage by increasing pigmentation in cells (Jimbow *et al.*, 1975). MITF is the master regulator of melanocyte differentiation. It is a transcription factor that regulates the genes responsible for differentiation such as tyrosinase (D'Orazio and Fisher, 2011). Differentiation is important in melanocytes because it helps protect the cells from undergoing transformation and tumor formation. *In vitro* cultured cells have shown that treatment with G-1 shows a reduces levels of c-myc while increasing levels of both tyrosinase and MITF (Natale *et al.*, 2018).

To assess the possible impacts LNS8801 may have on these melanocytes in our TGS mouse model we collected ear and tail tissue samples from TGS mice at various timepoints throughout the study, protein lysates were prepared for western immunoblots. Our analyses showed that c-myc levels vary greatly in all samples throughout the entire study, but some conclusions could be made. For female TGS mice, an overall increase in c-myc levels in both vehicle and LNS8801 treated mice regardless of UV exposure was included. For male TGS mice, in the absence of UV, both vehicle and LNS8801 treated group showed an overall similar increase in c-myc levels over the 32-week treatment period. With UV exposure, the c-myc levels were similar in vehicle-treated group but lower in LNS8801treated TGS males. These results would indicate that males treated with LNS8801 experience higher levels of melanocyte differentiation than female mice.

Tyrosinase levels varied between UV and non-UV exposed mice. In mice not exposed to UV tyrosinase levels increased over the 32-week experiment. This may correlate with an increase in tumor burden (increased pigmented lesions thus more pigment producing cells) on the ears of the mice where samples were taken from. Melanomas in this animal model are highly pigmented and have been shown to have

tyrosinase in them. Both male and female mice in the non-UV exposed group also showed higher levels of tyrosinase in vehicle controls than animals treated with LNS8801. In mice exposed to UV only male mice treated with LNS8801 showed an increase in tyrosinase over time where females only had a slight decrease. Our findings did not confirm previous *in vitro* results (Natale *et al.,* 2018).

We also evaluated another melanocyte differentiation marker, MITF. UV radiation in combination with LNS8801 in both females had very little influence in MITF levels in females and a moderate effect in males. Males exposed to UV and treated with LNS8801 showed reduced levels of MITF over time but not as much as those given the vehicle. In the absence of UV, MITF levels decreased over the 32-week experiment regardless of sex. These results indicate that melanocyte differentiation decreased over time likely due to increased disease progression. Treatment with LNS8801 and subsequent activation of GPER was not be able to confirm the findings of previous studies.

It is important to note that in many of these results, there is a clear difference in outcome depending on the gender of the animal. GPER is a receptor that can be activated by the endogenous sex hormone estrogen, in females that undoubtedly has some modulations that affect the outcome. Female TGS mice have a higher basal level of estrogen than male TGS mice, while LNS8801 binds to GPER with a higher affinity than estrogen the amount of LNS8801 we used may not saturate all of the available GPER receptors in melanocytes and the remaining ones may then be activated by native estrogen. Exposure to UV radiation yielded varied results within the sexes of the mice. Only female TGS mice treated with LNS8801 did not exhibit significant tumor

progression over 32-weeks, we propose that UV exposure may raise the overall mutational burden in the mice that may promote the immune-responses in these mice as suggested by the increased IFN-γ levels. Using a transgenic model that spontaneously develops melanoma allows us to better simulate the disease progression in human compared to an allograft model where the tumors are formed by inoculation of homogenous tumor cells into the flanks of mice. Tumor progression in the TGS model mimics the natural progression of disease in humans thus, allows us to perform longitudinal studies to assess consequences in a long-term study.

FUTURE DIRECTIONS

In order for us to rigorously examine the protein markers we selected and propose mechanisms of action of LNS8801, a selected GPER agonist in our melanoma mouse model system, additional western blots will need to be performed. Other melanocyte differentiation and pigmentation markers also may be included in subsequent analyses. Throughout the studies we also collected tumor specimens for immunohistochemistry studies, we will use antibodies against protein markers examined by westerns including c-myc, tyrosinase and MITF. Hematoxylin and eosin staining should also be performed on formalin fixed liver sample to ensure there is no obvious toxicity due to treatment with LNS8801.

Since there was a difference in tumor burden progression between male and female mice further investigations are needed to elucidate the underlying mechanisms that mediate the differences. We confirmed the presence of GPER in our tissue samples collected before running subsequent western blots (Figure 19). In future studies higher levels of LNS8801may be used to saturate the GPER receptors and overcome the beneficial differences detected in female mice. Possible mutational burden imposed by UV may be determined to ascertain the contribution to better responses in treatment.

Clinical trials of LNS8801 in combination with immune checkpoint blockade, anti-PD-1 are already ongoing. As another future study we could use LNS8801 in combination with anti-PD-1 in our TGS mouse model to see if we get similar results as those reported in the human clinical trial. The use of compounds, such as LNS8801, that take advantage of naturally occurring pathways and have low toxicity could prove beneficial in combination with other therapies.

REFERENCES

Arias-Pulido, Hugo, et al. "GPR30 and estrogen receptor expression: new insights into hormone dependence of inflammatory breast cancer." *Breast cancer research and treatment* 123.1 (2010): 51-58.

Bannai, Shiro. "Exchange of cystine and glutamate across plasma membrane of human fibroblasts." *Journal of Biological Chemistry* 261.5 (1986): 2256-2263.

Battaglia, Giuseppe, and Valeria Bruno. "Metabotropic glutamate receptor involvement in the pathophysiology of amyotrophic lateral sclerosis: new potential drug targets for therapeutic applications." *Current opinion in pharmacology* 38 (2018): 65-71.

Benavides, Fernando, et al. "The hairless mouse in skin research." *Journal of dermatological science* 53.1 (2009): 10-18.

Bologa, Cristian G., et al. "Virtual and biomolecular screening converge on a selective agonist for GPR30." *Nature chemical biology* 2.4 (2006): 207-212.

Brash, Douglas E., et al. "A role for sunlight in skin cancer: UV-induced p53 mutations in squamous cell carcinoma." *Proceedings of the National Academy of Sciences* 88.22 (1991): 10124-10128.

Brunsing, Ryan L., and Eric R. Prossnitz. "Induction of interleukin-10 in the T helper type 17 effector population by the G protein coupled estrogen receptor (GPER) agonist G-1." *Immunology* 134.1 (2011): 93-106.

Chen, Jin-Ran, et al. "Transient versus sustained phosphorylation and nuclear accumulation of ERKs underlie anti-versus pro-apoptotic effects of estrogens." *Journal of Biological Chemistry* 280.6 (2005): 4632-4638.

Chen, Suzie, et al. "Commitment of mouse fibroblasts to adipocyte differentiation by DNA transfection." *Science* 244.4904 (1989): 582-585.

Chimento, Adele, et al. "GPER agonist G-1 decreases adrenocortical carcinoma (ACC) cell growth in vitro and in vivo." *Oncotarget* 6.22 (2015): 19190.

Colón-Teicher, Luz, et al. "Genomic sequences capable of committing mouse and rat fibroblasts to adipogenesis." *Nucleic acids research* 21.9 (1993): 2223-2228.

Dackiw, Alan PB, et al. "Adrenal cortical carcinoma." *World journal of surgery* 25.7 (2001): 914.

Dankort, David, et al. "Braf V600E cooperates with Pten loss to induce metastatic melanoma." *Nature genetics* 41.5 (2009): 544-552.

de Araújo, Érica SS, Dimitrius T. Pramio, and Ana CV Krepischi. "Role of CDKN2A Mutations and Other Relevant Genes in Melanoma Predisposition." *Brain Metastases from Primary Tumors, Volume 3*. Academic Press, 2016. 101-117.

De Gruijl, F. R. "Skin cancer and solar UV radiation." *European Journal of Cancer* 35.14 (1999): 2003-2009.

Demaria, Sandra, et al. "Ionizing radiation inhibition of distant untreated tumors (abscopal effect) is immune mediated." *International Journal of Radiation Oncology* Biology* Physics* 58.3 (2004): 862-870.

Dzwierzynski, William W. "Managing malignant melanoma." *Plastic and reconstructive surgery* 132.3 (2013): 446e-460e.

D'Orazio, John, and David E. Fisher. "Central role for cAMP signaling in pigmentation and UV resistance." (2011): 8-9.

Eller, Mark S., Mina Yaar, and Barbara A. Gilchrest. "DNA damage and melanogenesis." *Nature* 372.6505 (1994): 413-414.

Filardo, Edward J., et al. "Distribution of GPR30, a seven membrane–spanning estrogen receptor, in primary breast cancer and its association with clinicopathologic determinants of tumor progression." *Clinical cancer research* 12.21 (2006): 6359-6366.

Filardo, Edward J., et al. "Estrogen action via the G protein-coupled receptor, GPR30: stimulation of adenylyl cyclase and cAMP-mediated attenuation of the epidermal growth factor receptor-to-MAPK signaling axis." *Molecular endocrinology* 16.1 (2002): 70-84.

Fisher, Michael S., and Margaret L. Kripke. 1977. "Systemic alteration induced in mice by ultraviolet light irradiation and its relationship to ultraviolet carcinogenesis". Proc. Natl. Acad. Sci. USA 74 (1997): 1688–1692.

Foulds, Kathryn E., Masashi J. Rotte, and Robert A. Seder. "IL-10 is required for optimal CD8 T cell memory following Listeria monocytogenes infection." *The Journal of Immunology* 177.4 (2006): 2565-2574.

Gates, Frederick L. "On nuclear derivatives and the lethal action of ultra-violet light." *Science* 68.1768 (1928): 479-480.

Ha, Linan, Glenn Merlino, and Elena V. Sviderskaya. "Melanomagenesis: overcoming the barrier of melanocyte senescence." *Cell Cycle* 7.13 (2008): 1944-1948.

Hedrich, Christian M., and Jay H. Bream. "Cell type-specific regulation of IL-10 expression in inflammation and disease." *Immunologic research* 47.1-3 (2010): 185-206.

Jimbow, Kowichi, et al. "Mitotic activity in non-neoplastic melanocytes in vivo as determined by histochemical, autoradiographic, and electron microscope studies." *The Journal of cell biology* 66.3 (1975): 663-670.

Klein, Sabra L., and Katie L. Flanagan. "Sex differences in immune responses." *Nature Reviews Immunology* 16.10 (2016): 626.

Lauw, Fanny N., et al. "Proinflammatory effects of IL-10 during human endotoxemia." *The Journal of Immunology* 165.5 (2000): 2783-2789.

Lüscher, Christian, and Kimberly M. Huber. "Group 1 mGluR-dependent synaptic long-term depression: mechanisms and implications for circuitry and disease." *Neuron* 65.4 (2010): 445-459.

Lyons, Susan A., et al. "Autocrine glutamate signaling promotes glioma cell invasion." *Cancer research* 67.19 (2007): 9463-9471.

M Ribeiro, Fabiola, et al. "Group I metabotropic glutamate receptor signalling and its implication in neurological disease." *CNS & Neurological Disorders-Drug Targets (Formerly Current Drug Targets-CNS & Neurological Disorders)* 9.5 (2010): 574-595.

Manning, Brendan D., and Alex Toker. "AKT/PKB signaling: navigating the network." *Cell* 169.3 (2017): 381-405.

Maverakis, Emanual, et al. "Metastatic melanoma–a review of current and future treatment options." *Acta dermato-venereologica* 95.5 (2015): 516-527.

Maynard, Craig L., and Casey T. Weaver. "Diversity in the contribution of interleukin-10 to T-cell-mediated immune regulation." *Immunological reviews* 226.1 (2008): 219-233.

McCubrey, James A., et al. "Ras/Raf/MEK/ERK and PI3K/PTEN/Akt/mTOR cascade inhibitors: how mutations can result in therapy resistance and how to overcome resistance." *Oncotarget* 3.10 (2012): 1068.

Meldrum, Brian S. "Glutamate as a neurotransmitter in the brain: review of physiology and pathology." *The Journal of nutrition* 130.4 (2000): 1007S-1015S.

Ménard, Caroline, and Rémi Quirion. "Group 1 metabotropic glutamate receptor function and its regulation of learning and memory in the aging brain." *Frontiers in pharmacology* 3 (2012): 182.

Natale, Christopher A., et al. "Sex steroids regulate skin pigmentation through nonclassical membrane-bound receptors." *Elife* 5 (2016): e15104.

Natale, Christopher A., et al. "Activation of G protein-coupled estrogen receptor signaling inhibits melanoma and improves response to immune checkpoint blockade." *Elife* 7 (2018): e31770.

Norval, Mary. "The mechanisms and consequences of ultraviolet-induced immunosuppression." *Progress in biophysics and molecular biology* 92.1 (2006): 108-118.

Pollock, P. M., Cohen-Solal, K., Sood, R., Namkoong, J., Martino, J. J., Koganti, A., Zhu, H., Robbins, C., Makalowska, I., and Shin, S.-S. “Melanoma mouse model

implicates metabotropic glutamate signaling in melanocytic neoplasia”. *Nature genetics* 34(1), (2003):108-112.

Prossnitz, Eric R., and Matthias Barton. "The G-protein-coupled estrogen receptor GPER in health and disease." *Nature Reviews Endocrinology* 7.12 (2011): 715.

Revankar, Chetana M., et al. "A transmembrane intracellular estrogen receptor mediates rapid cell signaling." *Science* 307.5715 (2005): 1625-1630.

Sato, Hideyo, et al. "Cloning and expression of a plasma membrane cystine/glutamate exchange transporter composed of two distinct proteins." *Journal of Biological Chemistry* 274.17 (1999): 11455-11458.

Schlagbauer-Wadl, Hermine, et al. "Influence of increased c-Myc expression on the growth characteristics of human melanoma." *Journal of Investigative Dermatology* 112.3 (1999): 332-336.

Schönwasser, Dorothee C., et al. "Activation of the mitogen-activated protein kinase/extracellular signal-regulated kinase pathway by conventional, novel, and atypical protein kinase C isotypes." *Molecular and cellular biology* 18.2 (1998): 790-798.

Schwarz, Thomas. "Mechanisms of UV-induced immunosuppression." *The Keio journal of medicine* 54.4 (2005): 165-171.

Shin, Seung-Shick, et al. "Oncogenic activities of metabotropic glutamate receptor 1 (Grm1) in melanocyte transformation." *Pigment cell & melanoma research* 21.3 (2008): 368-378.

Siegel, Rebecca L., et al. "Colorectal cancer statistics, 2020." *CA: a cancer journal for clinicians* (2020).

Šitum, Mirna, et al. "The mechanisms of UV radiation in the development of malignant melanoma." *Collegium antropologicum* 31.1 (2007): 13-16.

Snapper, Clifford M., and William E. Paul. "Interferon-gamma and B cell stimulatory factor-1 reciprocally regulate Ig isotype production." *Science* 236.4804 (1987): 944-947.

Soehnge, Holly, Allal Ouhtit, and O. N. Ananthaswamy. "Mechanisms of induction of skin cancer by UV radiation." *Front Biosci* 2 (1997): D538-D551.

Sosman, Jeffrey A., et al. "Survival in BRAF V600–mutant advanced melanoma treated with vemurafenib." *New England Journal of Medicine* 366.8 (2012): 707-714.

Steuer, Conor E., and Suresh S. Ramalingam. "Tumor mutation burden: leading immunotherapy to the era of precision medicine." *J Clin Oncol* 36.7 (2018): 631-632.

Takayama, Hisashi, et al. "Diverse tumorigenesis associated with aberrant development in mice overexpressing hepatocyte growth factor/scatter factor." *Proceedings of the National Academy of Sciences* 94.2 (1997): 701-706.

Taylor, Stephen J., et al. "Activation of the β1 isozyme of phospholipase C by α subunits of the Gq class of G proteins." *Nature* 350.6318 (1991): 516-518.

Toews, G. B., P. R. Bergstresser, and J. W. Streilein. "Epidermal Langerhans cell density determines whether contact hypersensitivity or unresponsiveness follows skin painting with DNFB." *Journal of immunology* 124.1 (1980): 445-453.

Weißenborn, Christine, et al. "GPER functions as a tumor suppressor in MCF-7 and SK-BR-3 breast cancer cells." *Journal of cancer research and clinical oncology* 140.4 (2014): 663-671.

White, Laurens P. "Studies on melanoma: sex and survival in human melanoma." *New England Journal of Medicine* 260.16 (1959): 789-797.

Wood, Richard D. "DNA repair in eukaryotes." *Annual review of biochemistry* 65.1 (1996): 135-167.

Zhao, L., et al. "Metabotropic glutamate receptor 5 promotes proliferation of human neural stem/progenitor cells with activation of mitogen-activated protein kinases signaling pathway in vitro." *Neuroscience* 192 (2011): 185-194.

Zhu, Hua, et al. "Development of heritable melanoma in transgenic mice." *Journal of investigative dermatology* 110.3 (1998): 247-252.

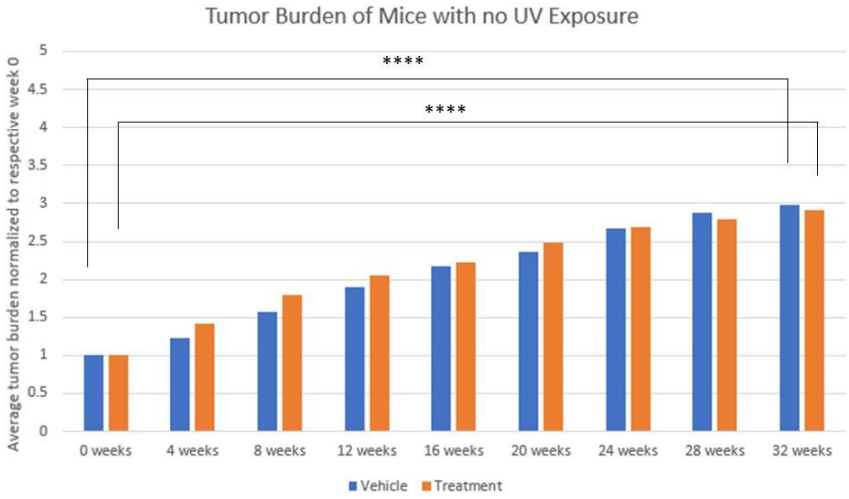

Figure 1: Average tumor burden for mice not exposed to UV radiation
Animals were treated three times a week for three consecutive days with either LNS8801 or vehicle. Images were taken with the small animal imaging system IVIS and tumor burden was calculated with ImageJ software provided the NIH. A (****) means a P value≤0.0001 showing statistical significance using a Bonferroni test comparing average tumor burden at week 0 to average tumor burden at week 32.

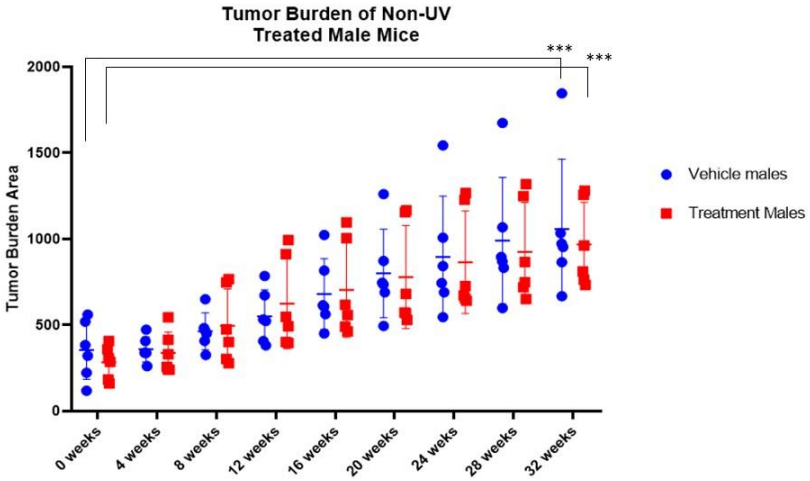

Figure 2: Total tumor burden for male mice not exposed to UV radiation
Animals were treated three times a week for three consecutive days with either LNS8801 or vehicle. Images were taken with the small animal imaging system IVIS and tumor burden was calculated with ImageJ software provided the NIH. A (***) means a P value≤0.001 showing statistical significance using a Bonferroni test comparing total tumor burden at week 0 to total tumor burden at week 32.

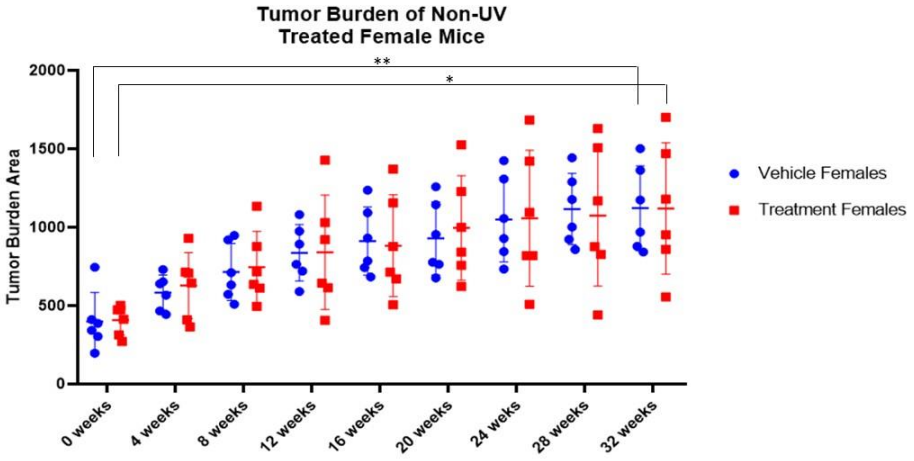

Figure 3: Total tumor burden for female mice not exposed to UV radiation
Animals were treated three times a week for three consecutive days with either LNS8801 or vehicle. Images were taken with the small animal imaging system IVIS and tumor burden was calculated with ImageJ software provided the NIH. A (*) means a P value≤0.05 and a (**) means a P value≤0.01 showing statistical significance using a Bonferroni test comparing total tumor burden at week 0 to total tumor burden at week 32.

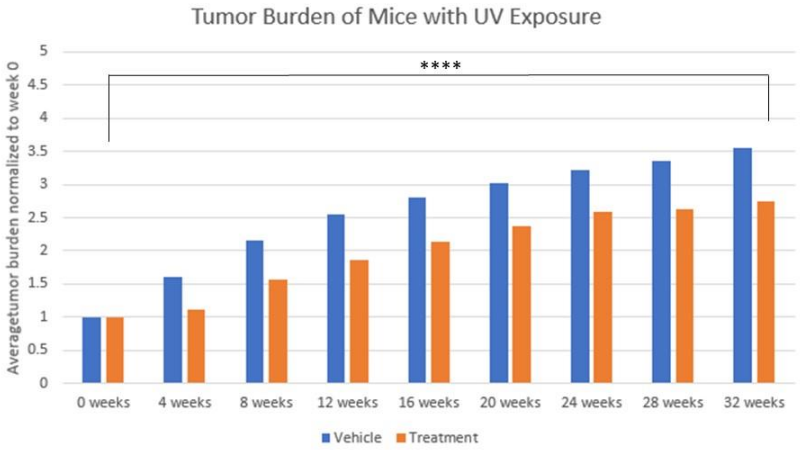

Figure 4: Average tumor burden for mice exposed to UV radiation
Animals were treated three times a week for three consecutive days with either LNS8801 or vehicle. UV exposure was once a week at a dosage of 30mJ/cm^2 . Images were taken with the small animal imaging system IVIS and tumor burden was calculated with ImageJ software provided the NIH. A (****) means a P value≤0.0001 showing statistical significance using a Bonferroni test comparing average tumor burden at week 0 to average tumor burden at week 32.

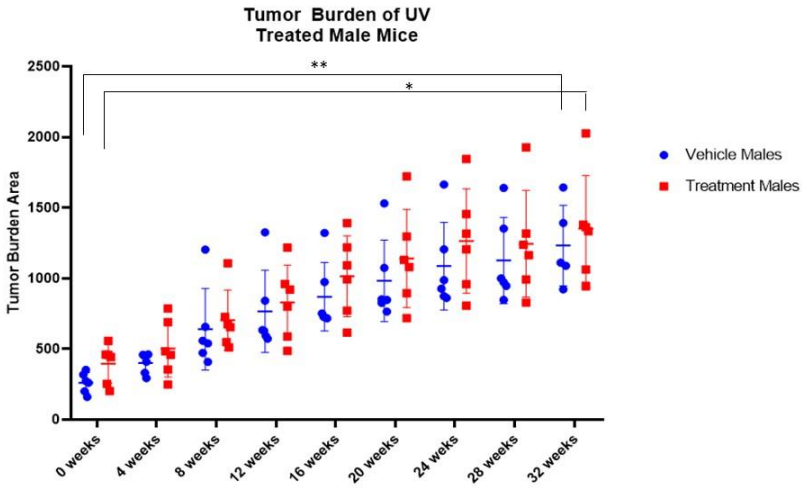

Figure 5: Total tumor burden for male mice exposed to UV radiation
Animals were treated three times a week for three consecutive days with either LNS8801 or vehicle. UV exposure was once a week at a dosage of 30mJ/cm^2 . Images were taken with the small animal imaging system IVIS and tumor burden was calculated with ImageJ software provided the NIH. A (*) means a P value≤0.05 and (**) means a P value≤0.01 showing statistical significance using a Bonferroni test comparing total tumor burden at week 0 to total tumor burden at week 32.

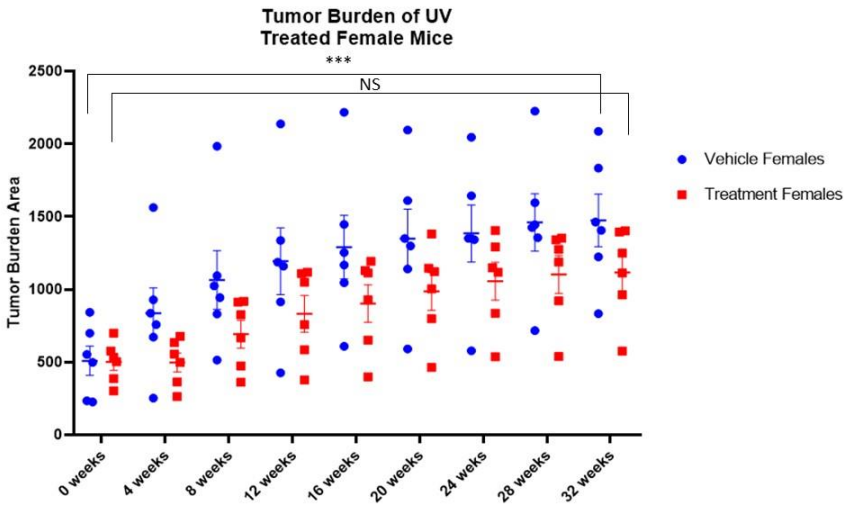

Figure 6: Total tumor burden for female mice exposed to UV radiation
Animals were treated three times a week for three consecutive days with either LNS8801 or vehicle. UV exposure was once a week at a dosage of 30mJ/cm^2 . Images were taken with the small animal imaging system IVIS and tumor burden was calculated with ImageJ software provided the NIH. A (***) means a P value≤0.001 showing statistical significance using a Bonferroni test comparing total tumor burden at week 0 to total tumor burden at week 32.

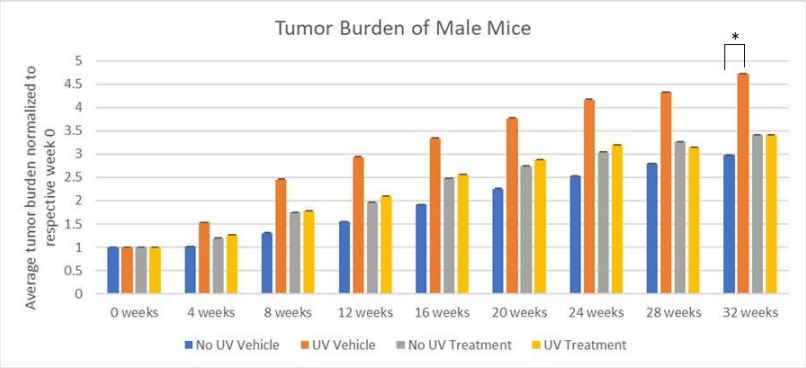

Figure 7: Average tumor burden for male mice
Animals were treated three times a week for three consecutive days with either LNS8801 or vehicle. UV exposure was once a week at a dosage of 30mJ/cm^2 . Images were taken with the small animal imaging system IVIS and tumor burden was calculated with ImageJ software provided the NIH. A (*) means a P value≤0.05 showing statistical significance using a Bonferroni test comparing total tumor burden week 32 between animals not exposed to UV and exposed to UV

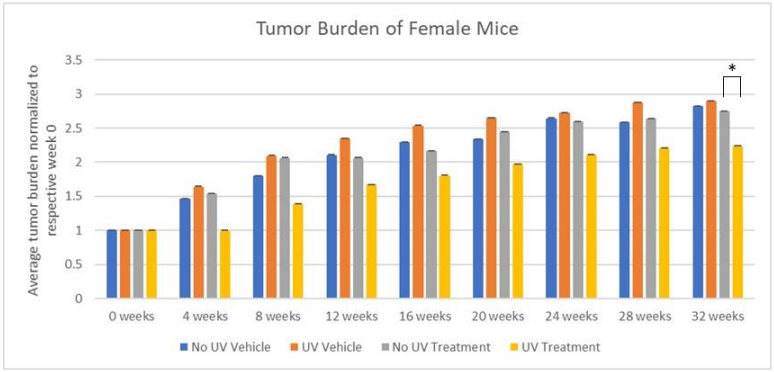

Figure 8: Tumor burden for female mice
Animals were treated three times a week for three consecutive days with either LNS8801 or vehicle. UV exposure was once a week at a dosage of 30mJ/cm^2 . Images were taken with the small animal imaging system IVIS and tumor burden was calculated with ImageJ software provided the NIH. A (*) means a P value≤0.05 showing statistical significance using a Bonferroni test comparing total tumor burden at week 32 between animals not exposed to UV and exposed to UV

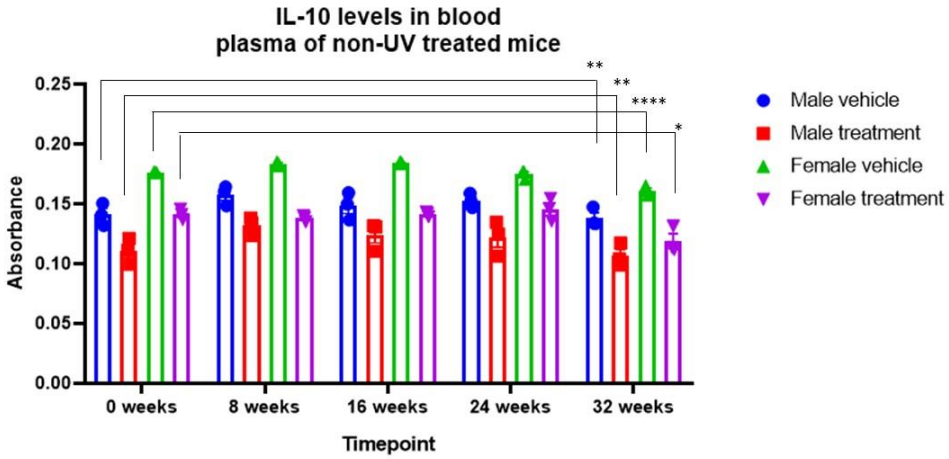

Figure 9: Average level of IL-10 found in the circulating blood plasma of mice not exposed to UV radiation
Animals were treated three times a week for three consecutive days with either LNS8801 or vehicle. Plasma was obtained from blood samples taken at designated timepoints and then an ELISA assay was performed. (*) means P value≤0.05, (**) P value≤0.01, (***) means a P value≤0.001, (****) P value≤0.0001 showing statistical significance using a Bonferroni test comparing average IL-10 levels from week 0 to week 32.

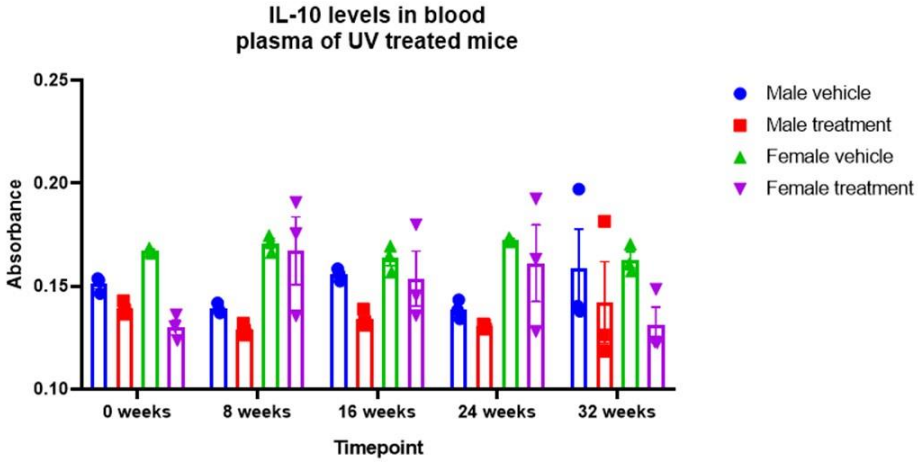

Figure 10: Average level of IL-10 found in the circulating blood plasma of mice exposed to UV radiation
Animals were treated three times a week for three consecutive days with either LNS8801 or vehicle. UV exposure was once a week at a dosage of 30mJ/cm^2 . Plasma was obtained from blood samples taken at designated timepoints and then an ELISA assay was performed. No statistical significance was found in IL-10 levels from week 0 to week 32.

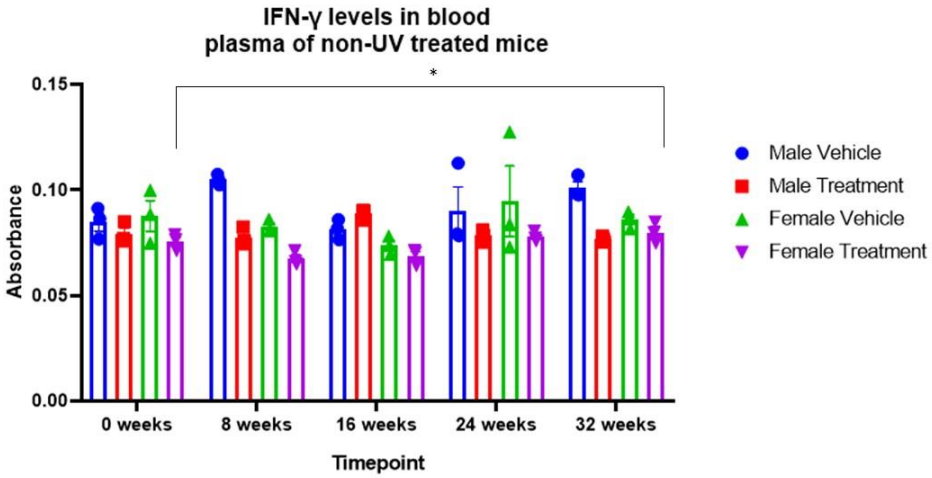

Figure 11: Average level of IFN-γ found in the circulating blood plasma of mice not exposed to UV radiation
Animals were treated three times a week for three consecutive days with either LNS8801 or vehicle. Plasma was obtained from blood samples taken at designated timepoints and then an ELISA assay was performed. (*) means P value≤0.05 showing statistical significance using a Bonferroni test comparing average IFN-γ levels from week 0 to week 32.

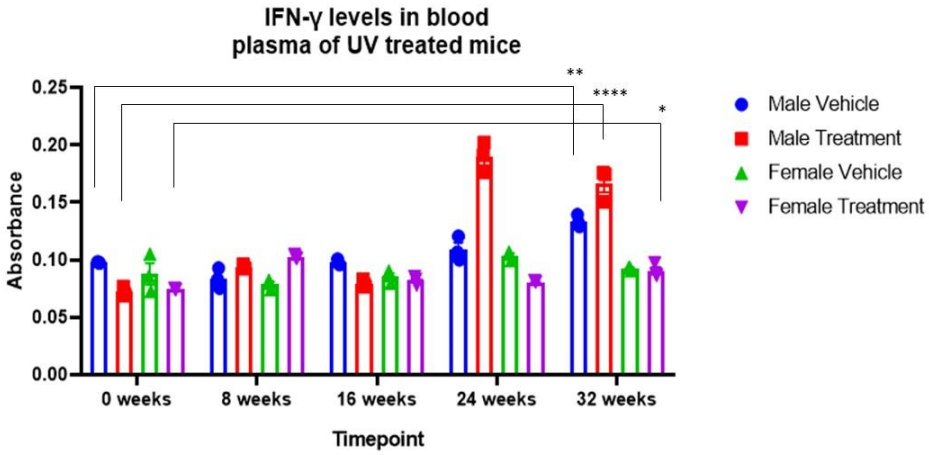

Figure 12: Average level of IFN-γ found in the circulating blood plasma of mice exposed to UV radiation
Animals were treated three times a week for three consecutive days with either LNS8801 or vehicle. UV exposure was once a week at a dosage of 30mJ/cm^2 . Plasma was obtained from blood samples taken at designated timepoints and then an ELISA assay was performed. (*) means P value≤0.05, (**) P value≤0.01, (****) P value≤0.0001 showing statistical significance using a Bonferroni test comparing average IFN-γ levels from week 0 to week 32.

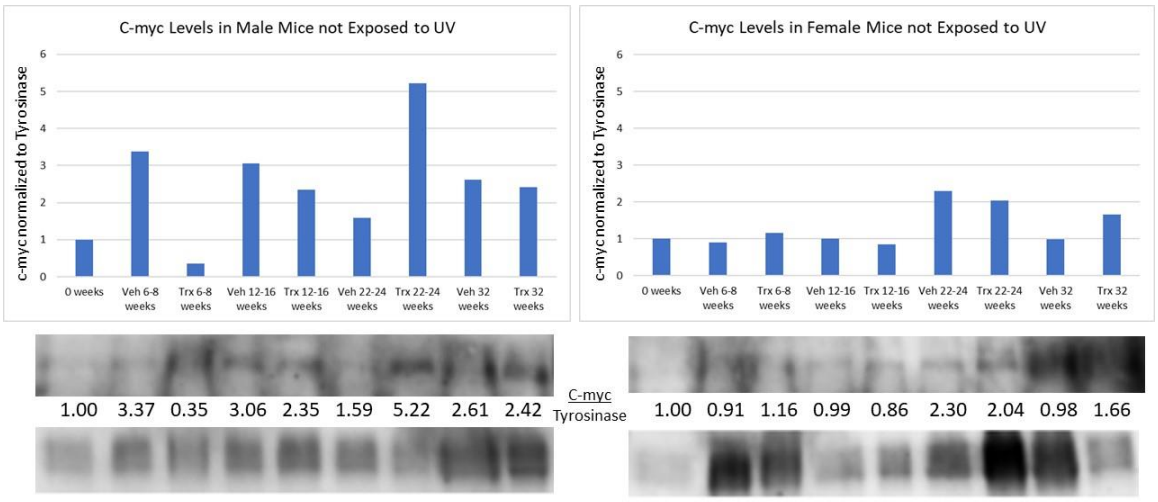

Figure 13: Expression levels of c-myc in non-UV exposed mice
Veh means vehicle treated, Trx means treated with LNS8801. Animals were treated three times a week for three consecutive days with either LNS8801 or vehicle. Tissue samples were collected from the ears and tail of mice at designated timepoints and then processed for protein lysate for Western Blot analysis.

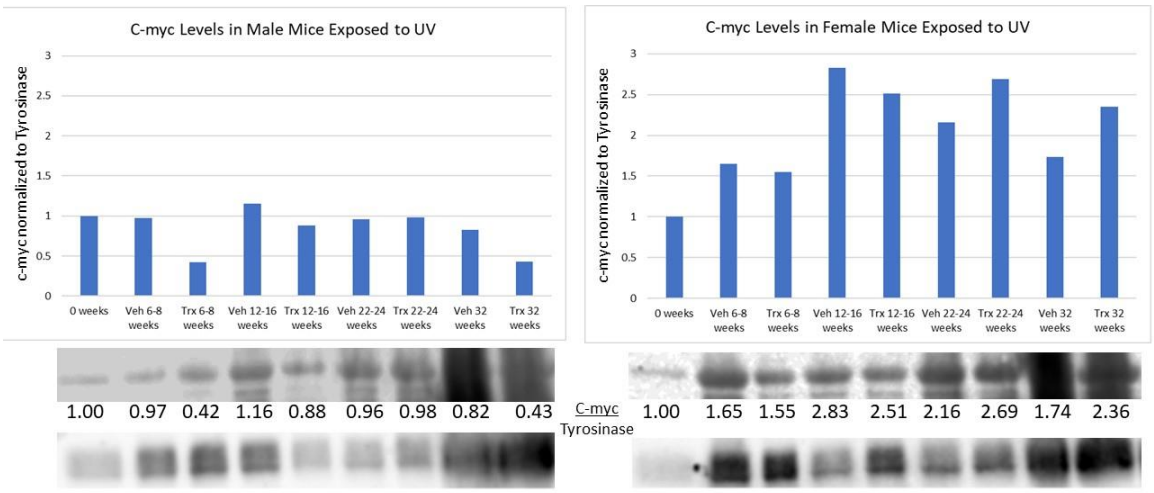

Figure 14: Expression levels of c-myc in UV exposed mice
Veh means vehicle treated, Trx means treated with LNS8801. Animals were treated three times a week for three consecutive days with either LNS8801 or vehicle. UV exposure was once a week at a dosage of 30mJ/cm^2 . Tissue samples were collected from the ears and tail of mice at designated timepoints and then processed for protein lysate for Western Blot analysis.

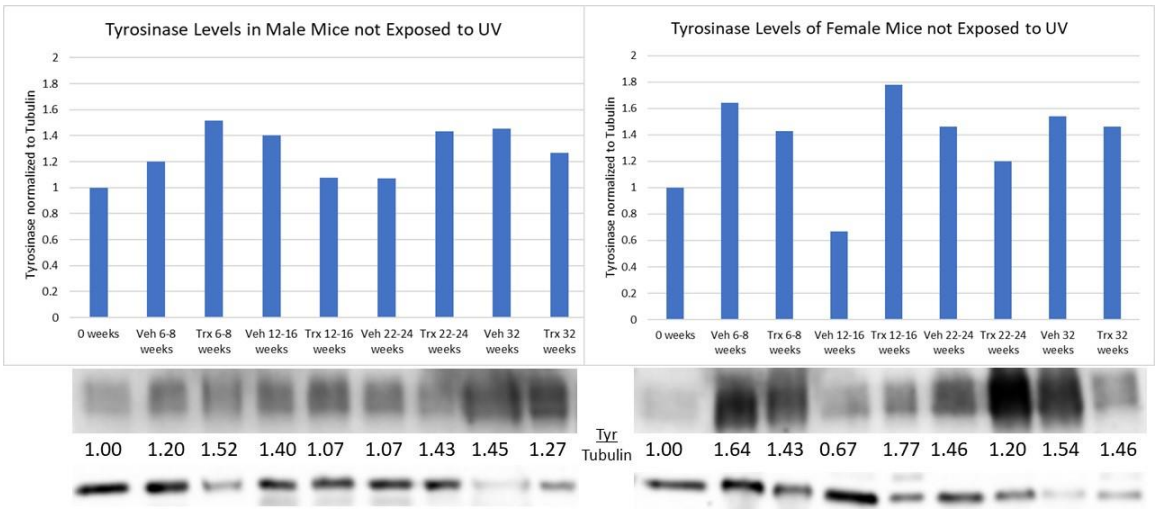

Figure 15: Expression levels of tyrosinase in non-UV exposed mice
Veh means vehicle treated, Trx means treated with LNS8801. Animals were treated three times a week for three consecutive days with either LNS8801 or vehicle. Tissue samples were collected from the ears and tail of mice at designated timepoints and then processed for protein lysate for Western Blot analysis.

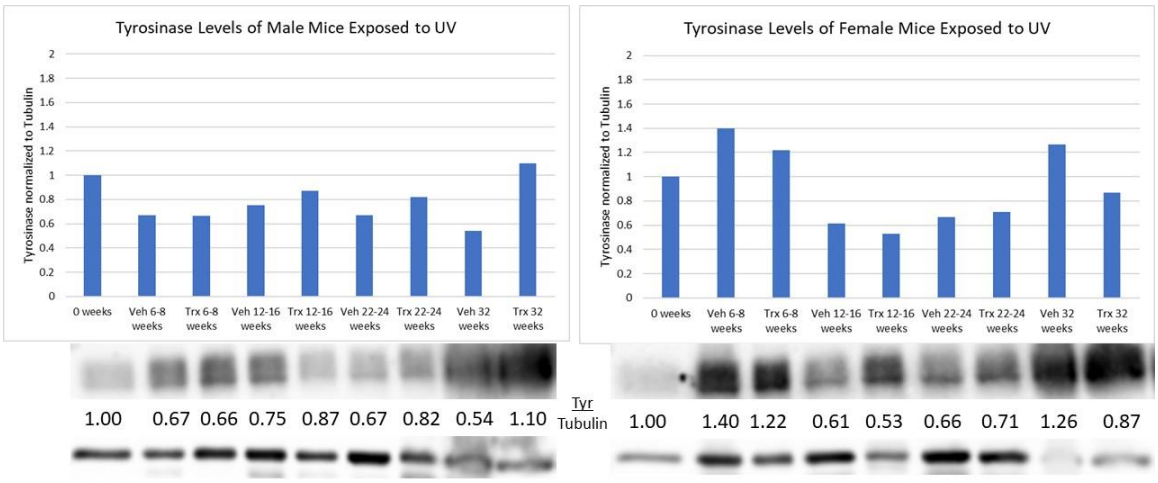

Figure 16: Expression levels of tyrosinase in UV exposed mice
Veh means vehicle treated, Trx means treated with LNS8801. Animals were treated three times a week for three consecutive days with either LNS8801 or vehicle. UV exposure was once a week at a dosage of 30mJ/cm^2 . Tissue samples were collected from the ears and tail of mice at designated timepoints and then processed for protein lysate for Western Blot analysis.

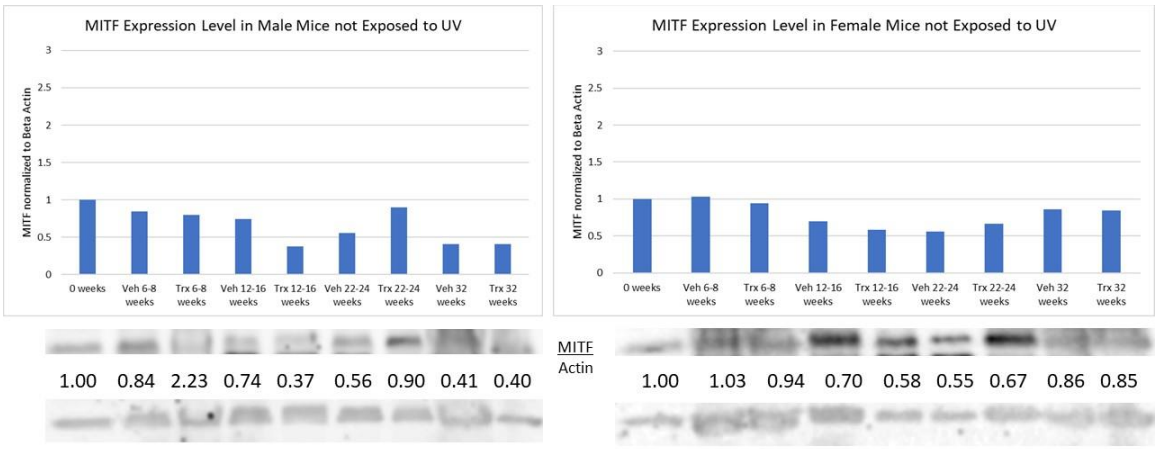

Figure 17: Expression levels of MITF in non-UV exposed mice
Veh means vehicle treated, Trx means treated with LNS8801. Animals were treated three times a week for three consecutive days with either LNS8801 or vehicle. Tissue samples were collected from the ears and tail of mice at designated timepoints and then processed for protein lysate for Western Blot analysis.

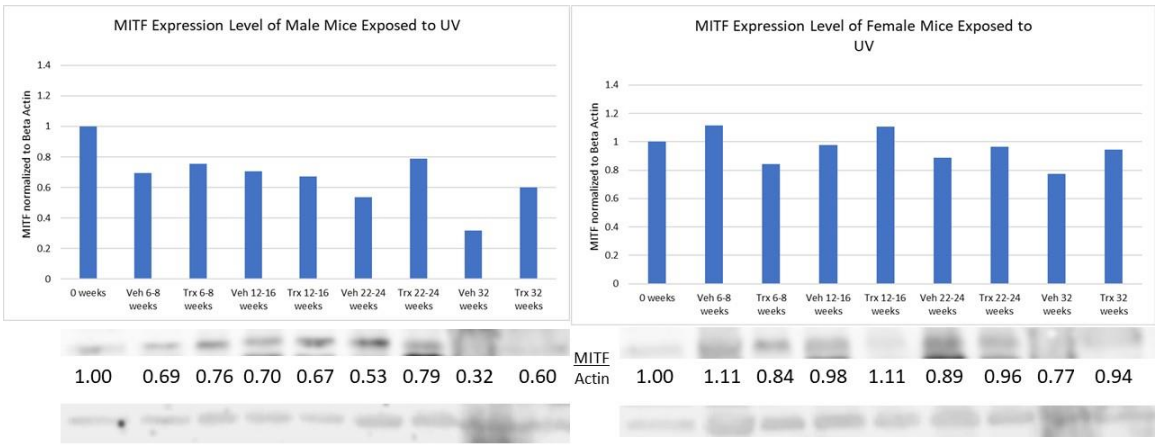

Figure 18: Expression levels of MITF in UV exposed mice
Veh means vehicle treated, Trx means treated with LNS8801. Animals were treated three times a week for three consecutive days with either LNS8801 or vehicle. UV exposure was once a week at a dosage of 30mJ/cm^2 . Tissue samples were collected from the ears and tail of mice at designated timepoints and then processed for protein lysate for Western Blot analysis.

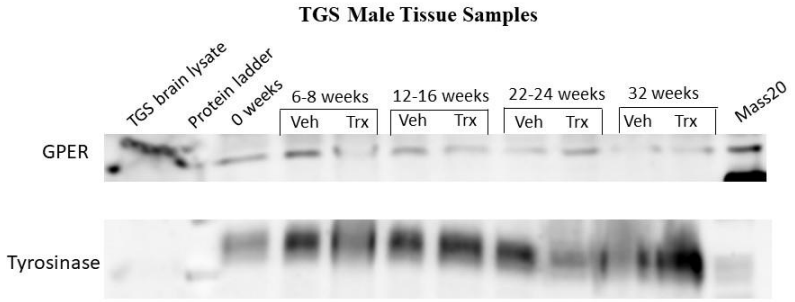

Figure 19: GPER is present in tissue samples
Western blot analyses for GPER showed the expression of GPER in male tissue samples collected throughout our study. Tyrosinase, a melanocyte specific protein, was used as a loading control. TGS brain tissue lysate and Mass20 cell lysate were used as positive controls for GPER. Mass20 was also a positive control for tyrosinase. Mass20 is a $GRM1^{+}$ mouse melanoma cell line. Veh=vehicle, Trx=treatment with LNS8801.